SPECIAL FIELD OF SPACE PROPULSION
TECHNISCHE UNIVERSITÄT MÜNCHEN
UNIV.-PROF.DR.-ING.OSKAR J. HAIDN

TERM PROJECT

Numerical Investigation of Cryogenic Propellants' Flashing Phenomenon

Author: **Usman Rana, B.Sc**
ID:03669800

Supervisor: Meng Luo, M.Sc

Issued: 18.10.2016
Submitted: 17.04.2017

Declaration of Authorship

Name: **Usman Rana**
ID: 03669800

I hereby declare that this thesis is my own work prepared without the help of a third party. No other than the listed literature and resources have been used. All sources transferred literally or analogously to this work have been labeled accordingly.

Additionally, I hereby certify that this thesis has not been underlain in any other examination procedure up to the present.

....
Date, Sign

Acknowledgements

I would like to thank my supervisor Mr. Meng Luo for his great support during this project. I appreciate his efforts and the time he invested in this project. In the last 6 months he was always keen to help me with his ideas, advice and discussions. Particularly in the last phase of this project we faced many problems and therefore we had to work almost regularly till midnight. This project was a great challenge. But we were able to accomplish it successfully.

Garching, April 17th 2017

Usman Rana

Abstract

In this term project a numerical study of cryogenic propellants' flashing phenomenon is conducted to investigate the behavoir of cryogenic propellants under vacuum condition. Two cryogenic fluids, i.e. liquid nitrogen and liquid oxygen are used in this study. Experiments conducted by the research associate Meng Luo from Chair of Turbomachinery and Flight Propulstion is used for the simulation validation.

Flashing occurs when a fluid undergoes a sudden depressurization, which may happen at the start-up of upper-stage rocket engine. Such depressurization process makes the fluid superheated. This superheated condition tiggers violent atomization and vaporization by nucleated boiling and bubble break up. Therefore the atomization of a flashing spray is quite different than the classical atomization, where aerodynamic forces and surface tension play a significant role.

In this study the Euler-Lagrange approach is applied in ANSYS FLUENT 17.2 for the flashing spray simulation. Since there is no model available for flashing spray in Fluent, a flashing evaporation model based on Adachi et al [1] and Zuo et al [2] is implemented into the Fluent Solver through User Defined Functions. The simulation results agree well with the experimental data.

Contents

List of Figures

List of Tables

1. Introduction

1.1. Flashing Phenomenon

Flashing refers to an atomization process, which produces a very fine spray. The physics of this kind of atomization is different than the normal mechanical atomization, which is caused by aerodynamic forces. The first researchers, who investigated this phenomenon were Ralph Brown and J.Louis York [7] in 1962. The authors defined a critical superheat, above which liquid shattering and rapid bubble growth can be observed in water and Freon-11. Furthermore droplet size, droplet velocities and spray pattern were analyzed. In the following years many researchers like Yildiz [8], Allen [9], Kitamura [10],Nghiem [11] and Park [12] contributed to increase the understanding of flashing phenomena through their experimental work. In addtion to this Lamanna [13] and Guatam [14] used cryogenic fluids instead of storable fulids and investigated their behavoir in superheated conditions. Valuable contributions to be mentioned from their research is, that spray behavoir is greatly influenced by low pressure regimes. Furthermore a domination of kinectic phase transition is observed in flashing evaporation in high superheated conditions.

Based on the work done by the metioned authors, further experimental research is conducted by the research associate Meng Luo from Chair of Turbomachinery and Flight Propulsion using cryogenic fluids like liquid nitrogen and liquid oxygen. The focus of his experimental work is to explore the spray pattern and thermal behavoir of spray, caused by flashing atomization. In this term project a numercial study is carried out using these experimental results for the validation process. Two cryogenic fluids are chosen for the numerical simulation liquid nitrogen and liquid oxygen. The aim of this study is to develope a simulation model of flashing atomization.

A model for flashing evaporation developed by Zuo et al [2] is used for the numerical simulation. This model is extended considering the significant role of radiation heat in the vacuum, which is of great importance for spacecraft engines. The commerical CFD code Ansys Fluent is used. Since there is no flashing evaporation model available in Ansys Fluent. A code is developed and implemented in this commercial software to simulate flashing evaporation.

2. Fundamentals

2.1. Theory of Flash Atomization

Flashing phenomena occurs, when a pressurized fluid undergoes a sudden depressurization, while it's temperature is maintained. The other reason for its occurence is, that the temperature of a liquid is increased above its saturation temperature, while the pressure remains unchanged. In both cases the liquid gets superheated and becomes metastable. This leads to rapid bubble growth, voilent atomization and evaporation due to thermodynamic non-equilibrium. In figure (2.1) a transition from subcooled liquid nitrogen to high superheated condition and then to stable saturation state is illustrated as observed in the experiments of Luo et al [3]. The point A represents the subcooled pressurized liquid nitrogen before injection. After the injection in a low pressure chamber, the fluid experiences a quasi-isothermal, isentropic pressure drop point B. At this state the fluid has become metastable and superheated and is currently in a thermodynamic non-equilibirium. Instantaneously rapid flash evaporation and atomization take place, so that a stable state point C can be reached.

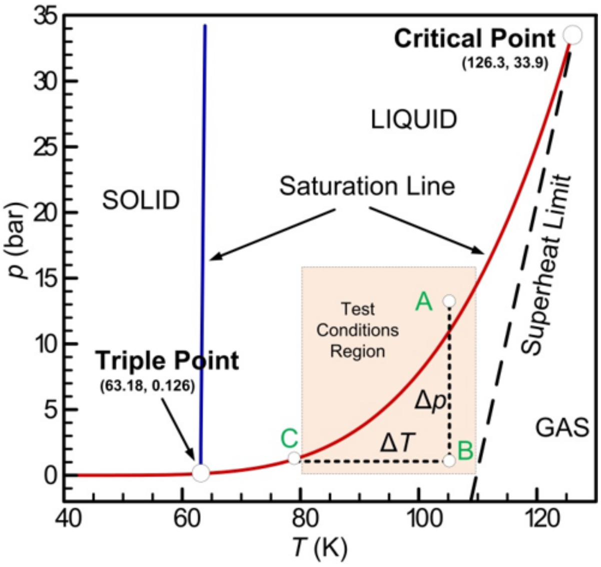

Figure 2.1.: P-T Diagram of Nitrogen [3]

The superheat of a liquid can be defined as a critical parameter which tiggers flashing. Two different definitions are used to characterize the superheat of a liquid. First is the difference between the injection temperature and boiling temperature corresponding to the surrounding pressure in the chamber as shown in equation (2.1).

The second definition represented by equation (2.2) is the ratio between the saturation pressure corresponding to the injection temperature and the surrounding pressure.

$$\Delta T = T_{inj} - T_b(p_\infty) \tag{2.1}$$

$$R_p = \frac{p_{sat}(T_{inj})}{p_\infty} \tag{2.2}$$

The level of superheat has a massive impact on the spray pattern. Such superheated sprays can be divided in three different catagories according to their superheat level. These catagories are mechanical atomization regime (low superheat), flashing onset regime (high superheat) and fully flashing regime (very high superheat). These catagoires are described in detail in section (5.1) .

Classical Nucleation Theory

According to the Classical Nucleation Theory the formation energy of a nucleas with a radius r can be determined with equation (2.3) [6]. The interfacial energy between the phases is represented by the first term. This energy is always positive as a result of formation of nucleus surface being energetically unfavorable. The difference in volume free energy between the phases is represented by the second term. In equation (2.4) G^* [6] is the maximum value of formation energy of a nucleas. This energy barrier G^* considered as a critical cluster should be overcome by a system to reach a new stable phase. If a nucleation cluster is langer than the critical nucleation cluster, it will grow and a nucleatin cluster smaller than the critical nucleater cluster will collapse.

In case of heterogeneous nucleation, the presence of additional material lowers the energy barrier and increases the rate of phase transtion see equation (2.5) [6].

$$\Delta G = 4\pi r^2 \sigma - \frac{4\pi}{3} r^3 \Delta\mu \tag{2.3}$$

$$\Delta G^* = \frac{16\pi(v_l)^2\sigma^3}{3[k_B T_{inj} ln(R_p)]^2} \tag{2.4}$$

$$\Delta G^{*het} = f(\phi)\Delta G^* < \Delta G^*, f(\phi) < 1 \tag{2.5}$$

2.2. Flash Atomization Model

A simplied modeling approach based on the classical D^2-theory is used. This modeling approach is adopted from Zuo et al [2]. It is assumed that the injected liquid disintegrates instantaneously at exit of the injector as a result of voilent atomization, which leads to spherically symmetric superheated droplets. In addtion to this immediate evaporation takes place and the surface temperature of the dropelts reaches the boiling temperature corresponding to the ambient pressure. Adachi's experimental correlation [1] is used for calculating the mass evporation $\dot{m}_f$ due to flashing.

$$\dot{m}_f = \frac{\alpha_s (T_p - T_b) A}{L(T_b)} \tag{2.6}$$

The heat transfer coefficient α_s is determined according to Adachi el al [1] as following.

$$\alpha_s = 13.8 (T_p - T_b)^{0.39} \;\; if\, (T_p - T_b \geq 25) \tag{2.7}$$

$$\alpha_s = 0.027 (T_p - T_b)^{2.33} \;\; if\, (5 \leq T_p - T_b \leq 25) \tag{2.8}$$

$$\alpha_s = 0.76 (T_p - T_b)^{0.2611} \;\; if\, (0 \leq T_p - T_b \leq 5) \tag{2.9}$$

The equation (2.6) only considers the internal heat transfer for the droplet mass vaporization due to the superheat. In this work the heat transfer from the surrounding to the droplet is taken into account. Since the external heat transfer play an important role in droplet mass vaporization process, this kind of superheated droplet vaporization is different from the vaporization coonsidered in classical D^2-theory in the following three ways

1. The surface temperature of a superheated droplet is assumed to be at the boling temperature. That means, the dropelt surface mass fraction Y^* approaches unity. As a result the mass transfer number B_M gets infinitely large, which would result erroneously in instantanouesly evaporation of the whole superheated dropelt.

2. The heat transfer from the surrounding to the dropelt surface only contributes to mass vaporization. It does not change that droplet temperature.

3. The flashing mass vaporization decreaces the amount of energy transfered from the surrounding.

Considering the above mentioned differeneces to the classical D^2-theory Zuo et al [2] proposed equation (2.10) for determinng the mass vaporization $\dot{m}_c$ resulting from the heat transfer from the surrounding to a superheated dropelt.

$$\dot{m}_c = 4\pi \frac{\lambda_{ref}}{c_{p,ref}} r_0 \frac{Nu}{1 + \dot{m}_f / \dot{m}_c} ln[1 + (1 + \frac{\dot{m}_f}{\dot{m}_c}) \frac{h_\infty - h_b}{L(T_b)}] \tag{2.10}$$

A reference temperature is used for the determing the properties e.g thermal conductivity λ_{ref}, heat capacity cp_{ref} and viscosity μ_{ref}. This reference temperature is calculated according to the one-third rule with equation (2.11).

$$T_{ref} = \frac{2}{3}T_b + \frac{1}{3}T_\infty \tag{2.11}$$

Massive evaporation due to high superheat leads to a blowing effect and as a result the boundary layer around droplet gets thicker.This influences the heat transfer from the surrounding. Considering the thickning of the boundary layer Stefan flow modification is used with a correction factor F_T for the standard Nusselt number Nu_0 according to Froessling correlation [15]. The modified Nusselt number Nu is determined as following.

$$Nu_0 = 2 + 0.552 Re^{1/2} Pr^{1/3} \tag{2.12}$$

$$Pr = \frac{\mu_{ref} c_{p,ref}}{\lambda_{ref}} \tag{2.13}$$

$$Re = \frac{\rho_\infty(\mid vd - vg \mid)D_d}{\mu_{ref}} \tag{2.14}$$

The correction factor F_T is calculated with equation (2.15) and transfer number B_T with equation (2.16) respectively.

$$F_T = (1 + B_T)^{0.7} \frac{ln(1 + B_T)}{B_T} \tag{2.15}$$

$$B_T = \frac{c_{p,ref}(T_\infty - T_b)}{L(T_b)} \tag{2.16}$$

Finally the modified Nusselt number Nu can be determined by using the correction factor F_T.

$$Nu = 2 + \frac{Nu_0 - 2}{F_T} \tag{2.17}$$

The total mass vaporation $\dot{m}_t$ according to Zuo et al [2] includes the mass vaporization caused by flashing $\dot{m}_f$ and the mass vaporization resulting from heat transfer from surrounding $\dot{m}_c$.

$$\dot{m}_t = \dot{m}_c + \dot{m}_f \tag{2.18}$$

The flash atomization model developed by Zuo et al does not consider the heat radiation from the surrounding to the liquid droplet. Since radiation plays a significant role in the vaccum, therefore it can not be neglected for vaporization process in spacecraft engines. Considering the purpose of this study, which is to develope a numerical simulation to investigate the flashing phenomena occuring in spacecraft engines. Radiative heat transfer from chamber wall to the droplet surface is taken into account and the flash atomization model is extended as following.

It is assumed that similar to conductive heat transfer from surrounding the radiativ heat transfer also does not change the droplet temprature. It only contributes to vaporize the mass at the surface of the droplet. Futher simplication is that the absorption coefficient α is 1 for both cryogenic propellants,used in this study.

$$\dot{m}_t = \dot{m}_c + \dot{m}_f + \dot{m}_r \tag{2.19}$$

with mass vaporizaton due to radiative heat transfer $\dot{m}_r$

$$\dot{m}_r = \frac{\sigma A_d \alpha (T_{wall}^4 - T_b^4)}{L(T_b)} \tag{2.20}$$

As previously mentioned the heat transfer from the surrounding, which includes radation and conduction, has no influence on the droplet temperature.That means that the droplet temperature is decoupled from the heat transfer from the surrounding. As a result only mass vaporization due to flashing changes the droplet temperature as shown in equation (2.21) .

$$\frac{\partial T_d}{\partial t} = -\frac{\dot{m}_f L(T_b)}{c_{p_d} m_d} \tag{2.21}$$

The energy source term to the gas is determined with equation equation (2.22).The reference Temperature T_{ref} is 298.15 K.

$$E = \dot{m}_t cp_d(T_p - T_{ref}) - (\dot{m}_r + \dot{m}_c)(L(T_b) - cp_g(T_b - T_{ref}) + cp_p(T_b - T_{ref})) \tag{2.22}$$

2.3. Numerical Approach

2.3.1. Conservation Equations

Conservation equations are used to calculate the fluid velocity and other properties for instance pressure, density, temperature and energy. Following fundamental physical laws are applied in the conservation equations. The fluid is treated as a continuum and molecular structure and motions at length scale of about $1\mu m$ are neglected.

1. Conversation of mass (equation (2.23))
2. Conversation of momentum (equation (2.24))
3. Conversation of energy (equation (2.25))

$$\frac{\partial \rho}{\partial t} + \nabla(\rho \vec{v}) = S_m \tag{2.23}$$

$$\frac{\partial u_i}{\partial t} + \frac{\partial(u_i u_i)}{\partial x_j} = -\frac{1}{\rho}\frac{\partial p}{\partial x_i} + \frac{\nu \partial^2 u_i}{\partial x_j \partial x_j} \tag{2.24}$$

$$\frac{\partial(\rho E)}{\partial t} + \nabla(\vec{v}(\rho E + p)) = -\nabla(\sum_j h_j J_j) + S_h \tag{2.25}$$

2.3.2. Turbulence Modeling

Different methods are used for numerical simulation of turbulent flows. These methods are Direct Numerical Simulation, Large Eddy Simulation and Reynolds- averaged Navier-Stockes. These methods differ from each other in needed compuational capacity and time. Since Direct Numerical Simulation resolves the whole turbulent spectrum of a fluid and Large Eddy Simulation resolves partly the turbulent spectrum. RANS method is used in most enginnering applications. Because there is no need of such high resulotion of the turbulent spectrum. This method is sufficient enough for most engineering cases. For this reason the needed computational time and capactiy for a RANS simulation is many orders lower than DNS and LES. Considering this RANS method with $k-\varepsilon$ model is used in this study and a brief description of RANS is given in the following subsection.

Reynolds-averaged Navier-Stockes

The exact Navier-Stockes equation for momentum transport is shown in equation (2.26).

$$\frac{\partial u_i}{\partial t} + \frac{\partial(u_i u_j)}{\partial x_j} = -\frac{1}{\rho}\frac{\partial p}{\partial x_i} + \nu \frac{\partial^2 u_i}{\partial x_j \partial x_j} \tag{2.26}$$

The solution parameters in the exact Navier-Stockes equation for example velocity is decomposed into mean and fluctuating components in Reynolds-averaged-Navier-Stockes equation equation (2.27). The mean value of the velocity is $\bar{u}$ and $u^{'}$ is its fluctuating component. By substituting the soluation parameters of the exact Navier-Stockes equation for expample velocity and pressure with a mean and fluctuating components the Reynolds-averaged Navier-Stockes equation can be derived as represented by equation (2.28).

$$u_i = \bar{u}_i + u^{'} \tag{2.27}$$

$$\frac{\partial \bar{u}_i}{\partial t} + \frac{\partial(\bar{u}_i \bar{u}_j)}{\partial x_j} + \frac{\partial(\overline{u_i^{'} u_j^{'}})}{\partial x_j} = -\frac{1}{\rho}\frac{\partial \bar{p}}{\partial x_i} + \nu \frac{\partial^2 \bar{u}_i}{\partial x_j \partial x_j} \tag{2.28}$$

The Reynolds-averaged Navier-Stockes momentum equation contains an additional term, third term in equation (2.28) , compared to exact Navier-Stockes equation (2.26). This addtional term is called Reynolds stresses and represents the turbulence effect. It consists of 6 unkown parameter. Therefore additional relationships are required between the unknown paramters in Reynolds stresses and the known fluid parameters. Finding these relationships is the basis of turbulence modeling.

A common approach for modeling the Reynolds stresses is the Boussniq approximation, which assumes that there is a similarity between the Reynolds stresses and the molecular shear stresses. In a newtonian fluid the molecular shear stresses are proportional to the fluid viscosity and the gradient of its mean velocity. On the analogy of this the turbluent stresses are assumed to be proportional to turblent viscosity and the gradient of fluid's mean viscosity. With this Assumption the 6 unkown parameter of the Reyolds stresses can be replaced by the turbulent visocisty to close the Reynolds-averaged Navier-Stockes equation (2.28).Turbulence model based on the Boussinesq approximation are called Eddy Viscosity Models.The other way of modeling the Reynolds stresses term is Reynolds stress equation model also referred to as second order closure model.For a deeper understanding of these turbulence models study of literature [16] is recommened. A brief description of Eddy Viscosity Model is given as following, since the two equation k-ε model is used in this study. The Eddy Viscosity Models are classified according to the number of differential equations used for modeling of Reynolds stress term.

1. Zero-equation model or alegbraic model (Prandtl's mixing-length concept)
2. One-equation model (Spalart-Allmaras S-A)
3. Two-equation model (k-epsilon and k-omega)

The algebraic model is not suitable for most engineering applications. But it is able to deliver very accurate results for wall-bounded, attached flow flieds, which have very small pressure gradients. In camparions to this the one-equation turbulenz model like Spalart-Allmaras uses a transportation equation for one characteristic variable, which describes the essential properties of the turbulenz. In most cases this transported charachteristic variable contains information about the total turbulent kinectic energy k. But this information is not sufficient enough to describe the turbulent structures precisely. Therefore further turbulent models like k-epsilon and k-omega were developed, which are most commonly used turbulence models in engineering applications due to their robustness, economy and reasonable computational capacity and time need for simulation. Since these models are most commonly used in engineering application a brief description of these models is given in the following subsections.

k-ε Model

It is assumed in this model, that that flow is fully turbulent and the effects of turbulent viscosity are not considered. As a result this model is only applied for fully turblent flow flieds. In comparison to one-equation model the k-ε model uses two transportation equations, one for the turbulence kinectic energy k equation (2.29) and the other for the dissipation rate ε equation (2.30) . As over the years weakness of this model have become known, many modifications have been introduced since then for example RNG k-ε model and realizable k-ε model. These models contain further modifications especially in the transportation equation of dissipation rate. The terms C represent the turbulence model constant, G the generation of turbulence kinectic energy, S the user defined source terms and Y the constribution of the fluctuating dilatation in compressible turbulence to overall dissipation rate [5].

$$\frac{\partial(\rho k)}{\partial t}+\frac{\partial(\rho k u_i)}{\partial x_i}=\frac{\partial}{\partial x_j}((\mu+\frac{\mu_t}{\sigma_k})\frac{\partial k}{\partial x_j})+G_k+G_b-\rho\varepsilon-Y_M+S_k \tag{2.29}$$

$$\frac{\partial(\rho \varepsilon)}{\partial t}+\frac{\partial(\varepsilon\rho u_i)}{\partial x_i}=\frac{\partial}{\partial x_j}((\mu+\frac{\mu_t}{\sigma_\varepsilon})\frac{\partial \varepsilon}{\partial x_j})+C_{1_\varepsilon}\frac{\varepsilon}{k}+(G_k+C_{3_\varepsilon G_b})-C_{2\varepsilon}\rho\frac{\varepsilon^2}{k}+S_\varepsilon \tag{2.30}$$

k-ω Model

The k-ω model is the other two equation model, which uses one partial differential equation for the turbulence kinectic k energy and one for specific rate of dissipation ω. This dissipation rate ω describes the dissipation of tubulence kinectic energy k into internal thermal energy. Unlike the k- ε model k-ω is modified for low-Reynolds effects, compressibility, and shear flow spreading.

$$\frac{\partial(\rho k)}{\partial t}+\frac{\partial(\rho k u_i)}{\partial x_i}=\frac{\partial}{\partial x_j}(T_k\frac{\partial k}{\partial x_j})+G_k-Y_k+S_k \tag{2.31}$$

$$\frac{\partial(\rho \omega)}{\partial t}+\frac{\partial(\rho\omega u_i)}{\partial x_i}=\frac{\partial}{\partial x_j}(T_\omega\frac{\partial \omega}{\partial x_j})+G_\omega-Y_\omega+S_\omega \tag{2.32}$$

For a deeper understanding of the k-ε and k-ω and other previously mentioned turblence models and their modifications study of the literature [5] is recommended.

2.3.3. Euler-Lagrange Approach

The Euler-Lagrange approach is applied for the calculation of multiphase flows. This method is used most commonly for sprays and fluids containing particles, for example solid particles in liquid flow field or liquid particle in a gaseous flow field. The Navier-Stockes equations are used for the calculation of the fluid phase equation (2.33). This phase is called as continous phase. This can be a liquid phase or a gaseous phase. The particles called as disperse phase are tracked in lagrangian frame and ordinary differential equations are applied to determine their trajectories equation (2.34) and equation (2.35). Three different regimes can be defined for the interaction between the fluid phase and disperse phase as following.

1. One-way coupling
2. Two-way coupling
3. Four-way coupling

In one-way coupling the continuous phase influences the disperse phase for example through turbulence and drag. In comparison to this the disperse does not influence the continuous phase. In two-way coupling the continuous phase influences the disperse phase, and the disperse phase also interacts with the continuous phase through source terms for instance energy, momentum and mass exchange. In four-way coupling in addtion to the influence of continuous phase on the disperse phase and interaction between continuous phase and disperse phase, there is also an interaction between the particles in the disperse phase. Since the two-way coupling is relevant for this study, a brief description of this method is given, by using the momentum exchange as an example.

Eulerian Phase

$$\frac{\partial(\rho_C u_C)}{\partial t} + \nabla(\rho_C u_C u_C) = -\nabla p + \nabla\tau + \rho_C g + F_i + S_d \tag{2.33}$$

Lagragian Phase

$$\frac{\partial x_d}{\partial t} = u_d \tag{2.34}$$

$$m_d \frac{\partial u_d}{\partial t} = \sum_i F_{di} \tag{2.35}$$

The source term from disperse phase to continuous S_d in equation (2.33) .

$$S_d = -\sum_i \rho d_i a d_i \left(\frac{\partial u_{di}}{\partial t} - g\right) \tag{2.36}$$

The figure (2.2) illustrates the principle of Euler-Lagrangian approach. As previously mentiond,the first step ist the calculation of the continuous phase for instance equation (2.33) without the source term S_d. Afterwards the particle trajectory will be determined with equation (2.34) and equation (2.35). The last step will be inclusion of source term from disperse phase equation (2.36) to continuous phase equation (2.33) and update of the new solution.

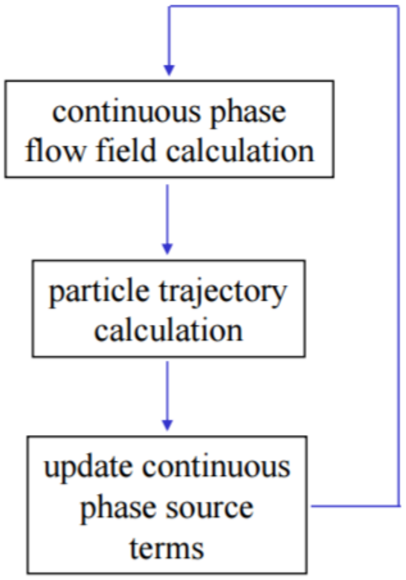
continuous phase flow field calculation
particle trajectory calculation
update continuous phase source terms

Figure 2.2.: Euler-Langrgian Model [4]

3. Flashing Vaporization Law

3.1. Heat and Mass Exchange Laws

In order to determine the source terms from the dispere phase to the continuous phase. The commercial code Ansys Fluent uses different heat and mass transfer relationships depending on the particle type and the particle temperature. For the particle type droplet following laws are available.

1. Inert Heating (Law 1)
2. Droplet Vaporization (Law 2)
3. Droplet Boiling (Law 3)

The figure (3.1) illustrates the conditions of activation of a specific heat mass exchange law.

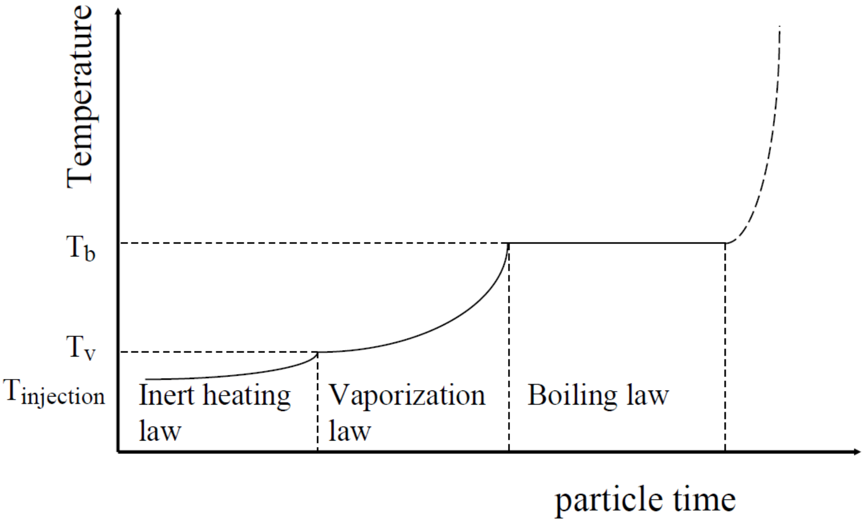

Figure 3.1.: Activation of Heat Mass Exchange Laws in Fluent [5]

The first law inert heating is activated, if the droplet temperature is under the vaporization temperature. A simple convective, radiative heat transfer balance to the droplet surface is used. Furthermore it is assumed that the droplet has no volative mass . After the droplet reaches the vaporization temperature, droplet vaporization law 2 is applied. For this law two different mass transfer models are used, diffusion controlled model and convection/diffusion controlled model. In diffusion controlled model the mass transfer happens due to vapor concentration difference between the particle surface and its surrounding. In case of high vaporization rates the influence of convective flow on the vaporization process is taken into account. By reaching the boling temperature law 3 is actived, which predicts the convective boiling rate and the vaporized mass. For this law Ansys Fluent assumes that the droplet temperature stays constant at the boiling temperature for the whole trajectory.

None of these standard available laws describes the heat mass exchange process of a superheated droplet, which happens due to the internal superheat of droplet. This flashing vaporization process is described in detail in section (2.2) of chapter (2). Considering the nonavailability of a heat mass exchange law, which describes the flashing vaporization process adequately. A new law named flash vaporization law is defined by using user defined functions. The figure (3.2) describes the activation process of new implemented flashing vaporization law in Ansys Fluent. In every iteration the current droplet temperature is determined. Depending on the current droplet temperature, Ansys Fluent either uses its standard laws, which are inert heating law, vaprization law and boiling law or activates the new implemented flash vaporization law. For the activation of this law the droplet temperature has to be above its boiling temperature. In case of activation of the flash vaporization law, the mass and energy source source terms are calculated according to the implemented code in flash vaporizaton law. These source terms are then added to the continuous phase. This process is repeated in every iteration, until the dropelt temperature sinks to its boiling temperature. In this case the boiling law is applied, and the heat and mass exchange is determined according to the boiling law. Further decay of droplet temperature leads to activation of vaporization law or inert heating law depending on the current droplet temperature.

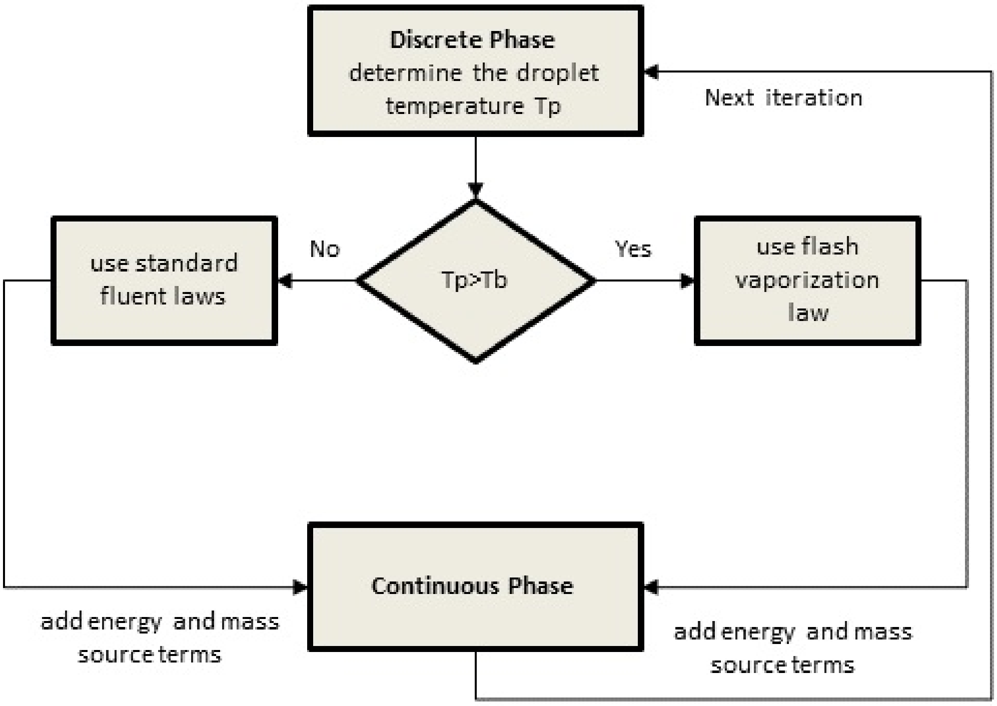

Figure 3.2.: Flashing Vaporization Law

3.2. User Defined Function

A user defined function is a code written in C language, which is used to enhance the standard available features in Ansys fluent. A UDF can be used to customize the material properties definitions, boundary condtions, energy and mass source terms, surface and volume reactions rates , etc. The flash vaporization law consists of several different user defined functions, used to determine the heat and mass exchange source terms according to the model of Zuo et al [2]. The UDF for flash vaporization law can be divided in four parts, DPM law, properties UDFs, DPM source and DPM switch.

3.2.1. DPM law

DPM law is used to customize mass, temperature, diameter and other properties of a dropelt according to its heat and mass exchange with surrounding. The following example of DPM law illustrates a UDF, which customizes the condensation model of a droplet depending on the local humidity. Further information about this example can be found in [17]. In the flash vaporization model the DPM law is used to determine the mass vaporization due to flashing, heat conduction and radiation from surrounding. This total vaporized mass is taken into account to calculate the new diameter, temperature and density of the droplet in every iteration step see appendix (B).

```
DEFINE_DPM_LAW(condenshumidlaw, p, coupled)
{
real area;
real mp_dot;
/* Get Cell and Thread from Particle Structure */
cell_t c = P_CELL(p);
Thread *t = P_CELL_THREAD(p);
area = 4.0 * M_PI * (P_DIAM(p) * P_DIAM(p));
/* Note This law only used if Humidity > 1.0 so mp_dot always positive*/
mp_dot = CONDENS * sqrt(area) * (myHumidity(c, t) - 1.0);
if (mp_dot > 0.0)
{
P_MASS(p) += mp_dot * P_DT(p);
P_DIAM(p) = pow(6.0 * P_MASS(p) / (P_RHO(p) * M_PI), 1./3.);
}
/* Assume condensing particle is in thermal equilibrium with fluid in cell */
P_T(p) = C_T(c,t);
}
```

3.2.2. Properties UDF

Properties UDFs are used to specify material properties such as density, viscosity, thermal conductivity, etc depending on the physical conditions. The following expample [17] of a property UDF calculates the cell viscosity according to the current temperature. In the flash vaporization model properties UDFs are used to deterime temperature dependend properties of the continuous phase for instance density, specific heat capacity, visocity, thermal conductitivity. Further information can be found in appendix (B).

```
DEFINE_PROPERTY(cell_viscosity,c,t)
{
real mu_lam;
real temp = C_T(c,t);
if (temp > 288.)
mu_lam = 5.5e-3;
else if (temp > 286.)
mu_lam = 143.2135 - 0.49725 * temp;
else
mu_lam = 1.;
return mu_lam;
}
```

3.2.3. DPM Source

DPM Source ist used to specify the droplet source terms from discrete phase to the continuous phase. By using this UDF the total source for instance energy source, mass source and momentum source are determined in a cell and then added to the continious phase. The following example [17] shows, how the source terms are determined in case of condensation. In flash vaporization model energy and mass sources are calculated according to the physics of flashing.

```
DEFINE_DPM_SOURCE(dpm_source, c, t, S, strength, p)
{
real mp_dot;
/* mp_dot is the mass source to the continuous phase
* (Difference in mass between entry and exit from cell)
* multiplied by strength (Number of particles/s in stream)
*/
mp_dot = (P_MASS0(p) - P_MASS(p)) * strength;
if (P_CURRENT_LAW(p) == DPM_LAW_USER_1)
{
/* Sources relevant to the user law 1:
* add the source to the condensing species
* equation and adjust the energy source by
* adding the latent heat at reference temperature
*/
S->species[h2o_index] += mp_dot;
S->energy -= mp_dot * P_INJECTION(p)->latent_heat_ref;
}}
```

3.2.4. DPM Switch

DPM switch is used for switching between different laws depending on a specific criteria, selected by the user. In the following example [17] DPM switch is used to switch between the user defined law, which is the DPM law and the standard available inert heating law, depending the criteria humidity. DPM switch is used in the flash vaporiaztion model to switch between the flash vaporization law and the boiling law depending on the droplet temperature see appendix (B)

```
DEFINE_DPM_SWITCH(dpm_switch, p, coupled)
{
cell_t c = P_CELL(p);
Thread *t = P_CELL_THREAD(p);
Material *m = P_MATERIAL(p);
/* If the relative humidity is higher than 1
* and the particle temperature below the boiling temperature
* switch to condensation law
*/
if ((C_UDMI(c,t,UDM_RH) > 1.0) && (P_T(p) < DPM_BOILING_TEMPERATURE(p, m)))
P_CURRENT_LAW(p) = DPM_LAW_USER_1;
else
P_CURRENT_LAW(p) = DPM_LAW_INITIAL_INERT_HEATING;
}
```

4. Experimental and Simulation Setup

4.1. Experimental Setup

Following experimental setup as shown in figure (4.1) is used to study the behavoir of cryogenic fluids for instance LN_2 and LOX. Main parts of the experimental setup are an optically accessible chamber with a single element jet injector, gas pressurization and cryogenic feed system, vacuum system, data acquisition system and optical diagnostic system. The dimensions of the chamber are 110mmx144mmx160mm.

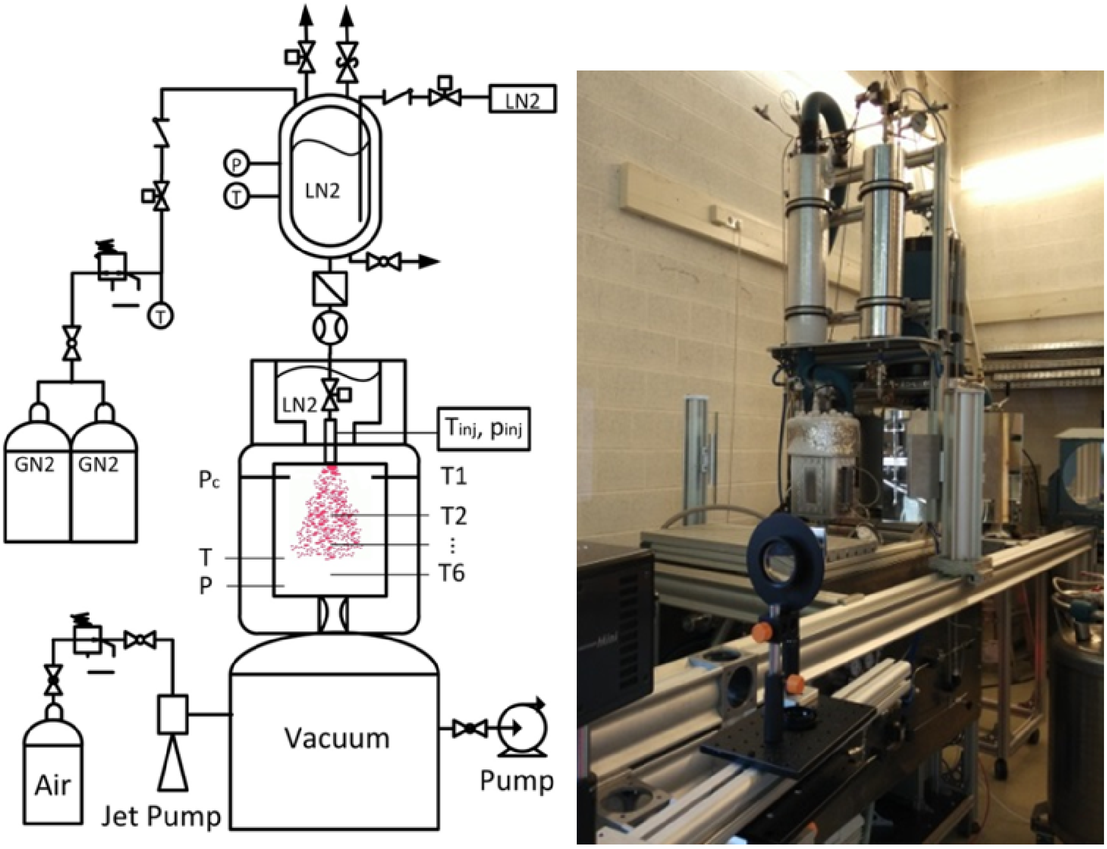

Figure 4.1.: Experimental Setup [6]

In figure (4.2) the optical diagonostic system is shown, used For the visualization of the spray caused by the flashing atomization. It consists of a light source with slit device, parabolic mirror, optical lens, and high-speed camera. Schlieren technique is applied for visualization process. Light-Emitting Diode referred as LEDs are used as the light source. The location of the slit device is at the foucs point of the first parabolic mirror ($f_2 = 3m$). The parabolic mirror is used to collect the slit light illumination, bundle it, so that parallel rays towards the plane mirror are produced and then reflected to the test region. The function of the second parabolic mirror is to collect the rays and the collimated light is focused on the high-speed camera (Photron FASTCAM Mini UX100) by convex lens. For the current experiments the resolution of the high speed camera is set at 1280x1024 at 4000fps with a shutter time of 20 μs. All nitrogen and oxygen experiments are conducted with injection pressure ranging from 9 bar to 11 bar. WIKA S10 and PMT-DS19 pressure sensors are used for the measurement of pressure inside the liquid nitrogen tank and the injection pressure. WIKA S10 pressure sensor has a working range of 0-25 bar and tolerance of ± 0.25 % and the PMT-DS19 sensor has a working range of 0-16 bar and toleranz of ± 0.25%. Further two pressure sensors WIKA A10,0-1 bar, ± 0.5% and WIKA S20, 0-1 bar, ± 0.25% are mounted in the chamber to measure the chamber pressure.

Due to the highly sensitivity of flashing phenomenon to the injection boundary conditions, the injector and the solenoid shutoff valve are immersed in the LN_2 and LOX bath to maintain constant injection temperature during the test. The temperature measurements are conduted by using thermocouple of type T. These thermocouples deliver stable and relatively precise performance under cryogenic conditions. In the current experimental set up a thermocouple is mounted every 20 mm along the injection axis, after calibrated them with LN_2 and LOX in the ambient pressure environment.

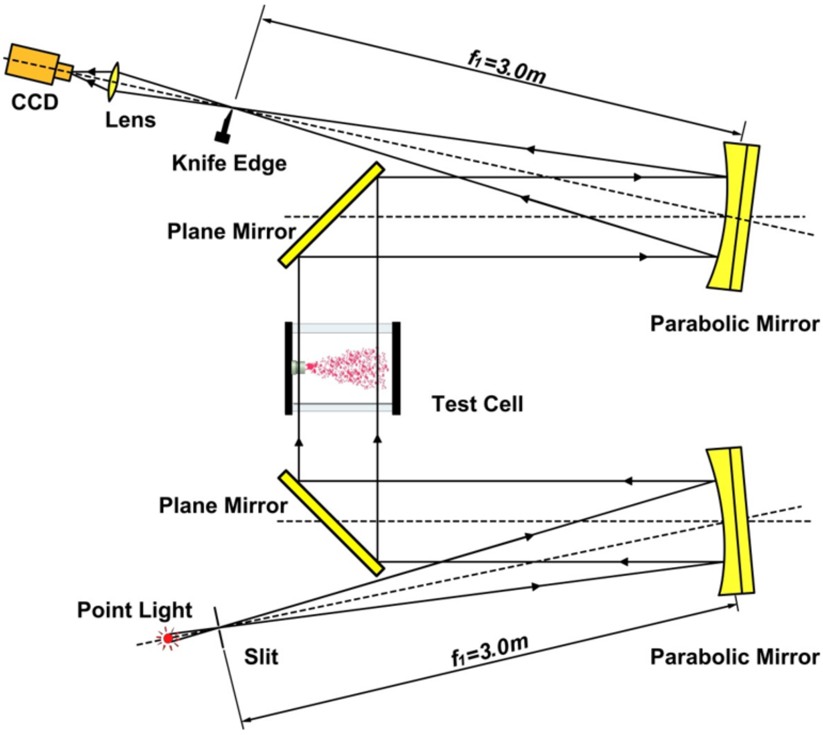

Figure 4.2.: Layout of Optical Setup [6]

4.2. Simulation Setup

The commerical software Ansys Fluent is used for the simulation of flash atomization. As previously mentioned Ansys Fluent does not have a proper model, which is able to describe the heat and mass exchange caused by the flashing phenomenon. Therefore a new heat and exchange model called flash vaporization law is implemented in Ansys Fluent. This model consists of several user defined functions as explained in section (3.2). The main parts are DPM law, properties user defined functions and DPM source. DPM law calculates the mass vaporization due to flashing, heat conduction and thermal radiation. According to the mass vaporization the new droplet diameter, temperature and density are determined in every iteration step. As the temperature of gas phase and droplets changes as result of mass vaporization, the temperature depended thermodynamic properties of the gas phase and the droplet are calculated by properties user defined functions. The energy and mass sources are added to the gas phase by using DPM source.

The gas phase is calculated in Eulerian frame and the liquid droplet are calculated in Lagrangian frame as explained in section (2.3.3). For the turbulence modeling $k-\varepsilon$ model with unsteady RANS method is used in combination with $1e^{-5}$s time step and PISO algorithm. Since this algorithm is very suitalbe for the calculation of transient flows. A structured mesh with 198000 cells as shown in figure (4.4) and figure (4.4) is used. The dimensions of the nummerical domain are 55mmx72mmx160mm, which is a quater of the chamber, used in the experiment. This domain is used with symmetric boundary condtions to reduce the computational time.

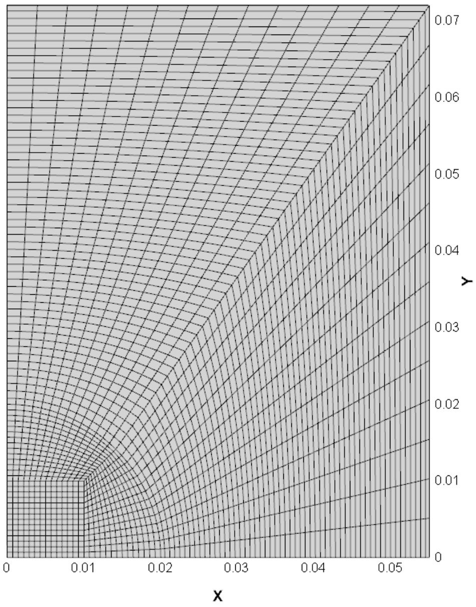

Figure 4.3.: Inlet or Outlet

Pressure inlet and pressure outlet are used as the inlet and outlet boundary conditions. Furthermore an instantaneous atomization after the injection is assumed, which represents the conducted tests in fully flashing regime as explained in section (5.1). Further simulation setup will be exlpained in chapter (5). Since each case has a different setup reagarding, dropelt diameter, injection velocity, injection pressure, injection angle etc.

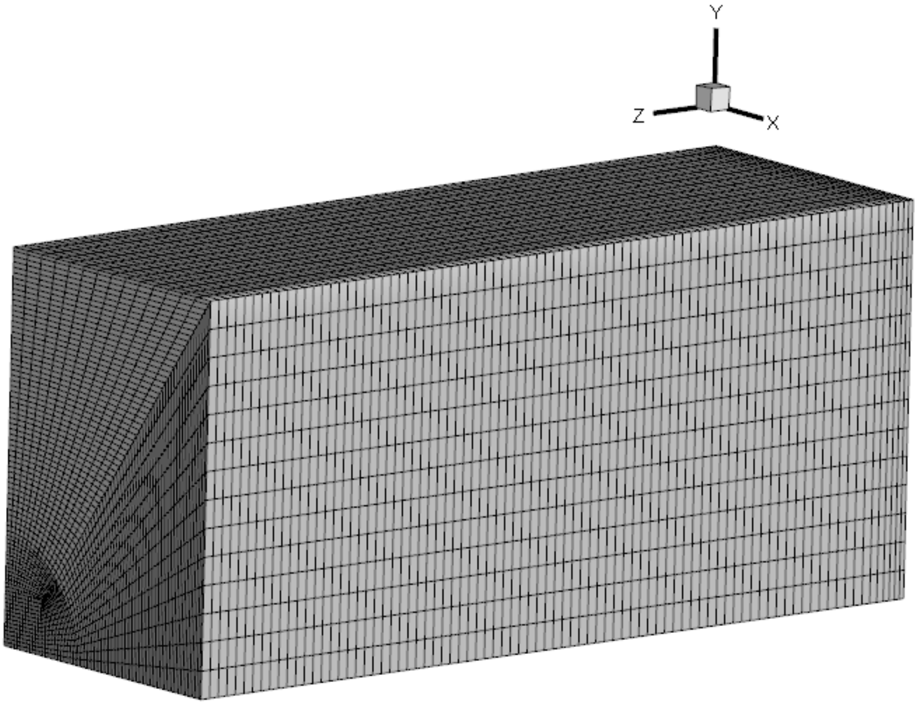

Figure 4.4.: Whole Mesh

5. Experimental and Simulation Results

5.1. Flashing evolution process

The experiments are conducted to study the behavoir of cryogenic propellants LN_2 and LOx in low pressure environment. In additon to this, the influence of level of superheat on the atomization process is also taken into account. Furthermore a new non-dimensional parameter ξ is proposed [6]. This parameter is based on the non-dimensional paramter χ [13],which is conditional and does not work well at higher injection temperatures. Therefore the new non-dimensional paramter ξ ist used to indicate the onset of partial flashing spray and fully flashing spray at high injection temperatures.

$$\xi = \frac{\Delta G^*}{k_B(T_{inj} - T_{sat(pc)})} = \frac{\Delta G^*}{k_B \Delta T} \tag{5.1}$$

In equation (5.1) $k_B T_{inj}$ is the thermal motion energy of the molecules and ΔG^* is the nucleation barrier. So the new non-dimensional parameter ξ [6] represents a energy barrier, which is a ratio of nucleation barrier to excessive thermal motion energy of the cluster. The excessive thermal motion energy can be considered as the difference between the initial thermal motion energy and the thermal motion energy at the final state of the fluid.

if the parameter ξ is large, the cluster is unable to overcome the nucleation barrier due to less excessive thermal motion energy. In case of smaller ξ the excessive energy is consumed by the active molecules through forming of numerous bubbles nucleas. This leads to keep local minimum energy state or achieve the global minimum energy state, through violent jet breakup,atomization and vaporization.

When the degree of superheat is low, the spray behaves as small liquid segments and then desintegrates into smaller droplets. This kind of atomization process corresponds to mechanical atomization(ξ >1). As the superheat increases, the spray jet shatters into more finer droplets. In this regime nucleated boiling starts to dominate the spray atomization. This refers to $\xi \sim 1$. In case of very high superheat level, a violent instantaneous atomization and vaprozation happen as a result of higher excessive thermal motion energy than the nucleation barrier (ξ<1).

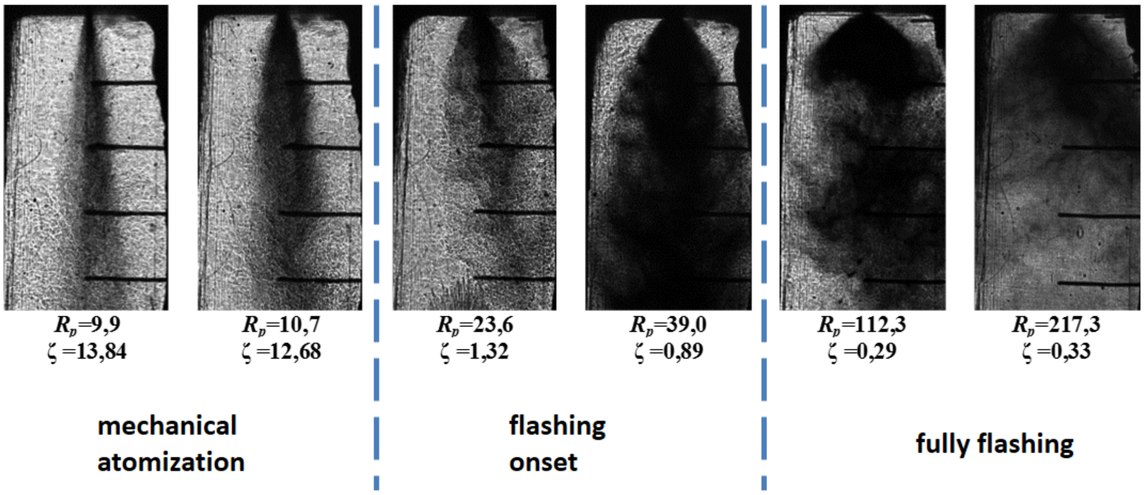

Figure 5.1.: LO_x Spray Regimes [6]

In figure (5.1) and figure (5.2) three different kind of atomization regimes depending on the propsed paramter ξ are shown. Mechanical atomization happens, if the non-dimensional parameter ξ is much higher than 1. In case of $\xi \sim 1$ flashing starts to dominate the atomization process and ξ<1 refers to fully flashing regime.

Futhermore it is observed, that a higher superheat increases the spray angel and produces a very fine spray. As the SMD of the spray deacreaes with higher superheat [18].

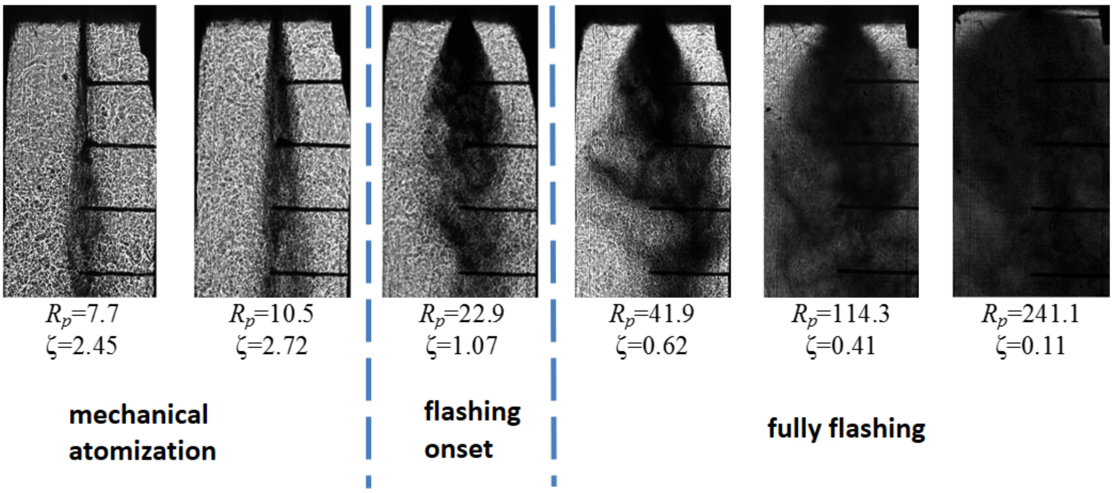

Figure 5.2.: LN_2 Spray Regimes [6]

5.2. Nitrogen and Oxygen Simulation

As already mentioned in section (4.2) the commerical simulation code Ansys Fluent is used for this study. Since Fluent does not provide any model, which is able to describe the flashing atomization. A new model named Flash vaporization law is implemented in Fluent through several User Defined Functions. Further information about this new model can be found in chapter (3). The code for this model is in appendix (B).
The Euler-Lagragian method is applied for the calculation of the spray. This method is called Discrete Phase Model (DPM) in Fluent. The unsteady RANS equations with a time step of $1e^{-5}$ s are used for the turbulence modeling. Since the turbulence effect on flashing phenomenon is expected to be very low, URANS method should be sufficient enough. The numerical domain used for this study is shown in figure (4.3) and figure (4.4). It consists of 198000 cells and represents the quater of the chamber, used in the experiment. Futhermore information about the numerical domain is given in section (4.2).

Following LN_2 and LO_x experiments as shown in table (5.1) and table (5.2) are chosen for the simulation.

Table 5.1.: LN_2 Case Experimental Data

$\dot{m}$	P_{inj}	P_c	T_{inj}	T_{satP_c}	ΔT	R_p	v	x/D
$6.1e^{-3}$ kg/s	9.97 bar	0.150 bar	97	64 K	33 K	41.9	44 m/s	82.7°

Table 5.2.: LO_x Case Experimental Data

$\dot{m}$	P_{inj}	P_c	T_{inj}	T_{satP_c}	ΔT	R_p	v	x/D
$7.5e^{-3}$ kg/s	10.7 bar	0.206 bar	116 K	77 K	42 K	39	38 m/s	101°

Basic Simulation Setup

Table 5.3.: Basic LN_2 Case Simulation Setup

Turbulence Model	Solver	Pressure Inlet	Pressure Outlet	Cell Pressure	Time step
$k-\varepsilon$	Pressure-based PISO	0.145 bar	0.145 bar	0.05 bar	$1e^{-5}$

Table 5.4.: Basic LO_x Case Simulation Setup

Turbulence Model	Solver	Pressure Inlet	Pressure Outlet	Cell Pressure	Time step
$k-\varepsilon$	Pressure-based PISO	0.201 bar	0.201 bar	0.05 bar	$1e^{-5}$

Solid cone is used as the injector with the setup as shown in table (5.5) and table (5.6). Since superheated sprays in fully flashing regime produce a very narrow range of droplet distribution [18]. Rosin-Rammler Distribution with minium droplet diameter of $10\mu m$, mean droplet diameter of $12\mu m$ and maximum droplet diamter of $18\mu m$ is chosen for both cases. The spread parameter for this distribution is 5. Furthermore instead of calculating every single droplet,which would be very time consuming, parcels approach is used. Since a sprays can consist of millions of droplet. These parcels contain serveral number of dropelts.

The total number of dropelts in a parcels can be a user given constant value, or determined depending on the user given diameter or the standard option, where the number of dropelts in a parcel is calculated by Fluent depending the mass flow, droplet diameter etc. The mass flow is $1.525e^{-3}$ kg/s for nitrogen case and $1.875e^{-3}kg/s$ for oxygen case. The used mass flow for both cases is quater of the total mass flow, used in the experiment. Since only quater of spray with symmetric boundary conditions is simulated to reduce the computational time. The injection temperature is same as in the experiment and the injection half angel of the spray is 41° for the nitrogen case and 50° for oxygen case, which is also similar to the angel measured in the experiment.

Table 5.5.: LN_2 Injector Setup

$\dot{m}$	Particle streams	Number of Parcels	T_{inj}	Particle diameter	Injection Angel
1.525^{-3} kg/s	150	Standard	97 K	Rosin-Rammler	41°

Table 5.6.: LO_x Injector Setup

$\dot{m}$	Particle streams	Number of Parcels	T_{inj}	Particle diameter	Injection Angel
$1.875e^{-3}$ kg/s	150	Standard	116 K	Rosin-Rammler	50°

5.2.1. Simulation Results and Discussion

The simulation starts with the assumption, that the liquid jet breaks up instantenously after the injection into very fine dropelts, representing the fully flashing regime as observed in the chosen experiments of superheat level of 33K and 42 K. A 3D view of the LN_2 spray simulation is illustrated in figure (5.3). As previously mentioned only quater of the spray with symmetric boundary condtions is simulated.

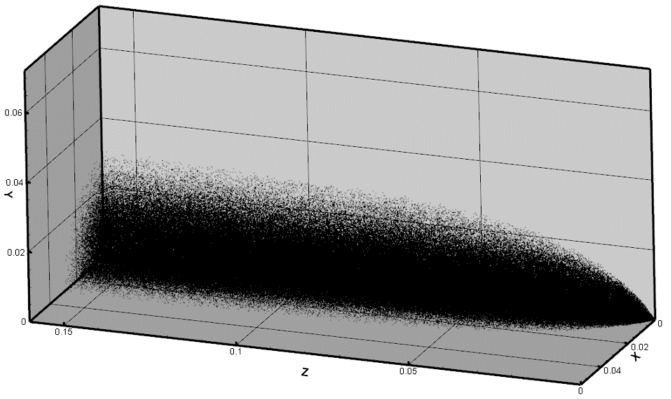

Figure 5.3.: 3D View of LN_2 Spray

This superheated spray reaches a stable equlibirium state downstream of the injector after a violent mass vaporization due to its superheat. Due to the massive evaporation, the evaporated vapor compresses the gas near the injector, which results in a pressure pike in the vincy of the injector orifice. After a short distance, several times of the nozzle diameter, the vaporized gas undergoes an isotropic expansion and the gas velocity increases with the static pressure decrease, as shown in figure (5.4) . As the superheat decreases futher downstream of the injector the pressure reaches a state of 0.15 bar for LN_2 case and 0.206 bar for LO_x case, which is the chamber pressure in the experiment.

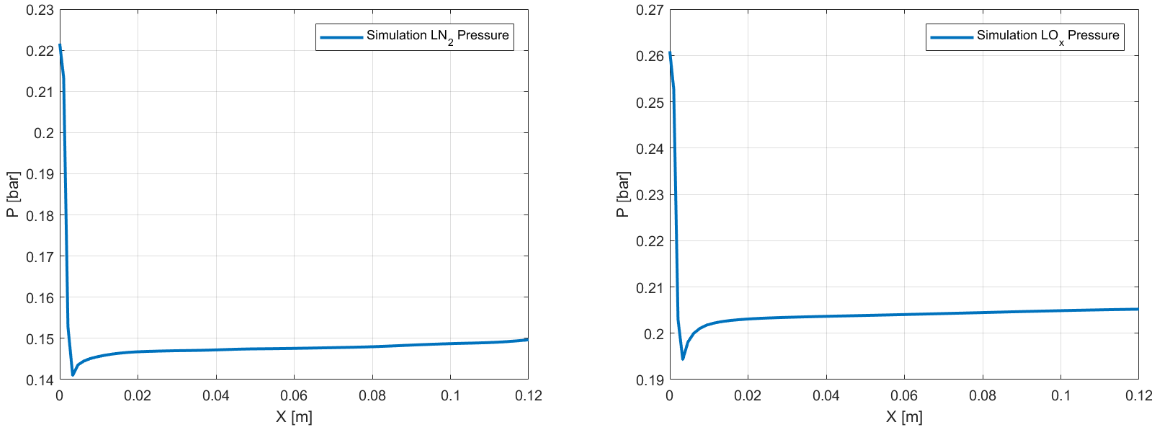

(a) LN_2 Gas Phase Pressure

(b) LO_x Gas Phase Pressure

Figure 5.4.: Effects of Mass Vaporization on Gas Phase Pressure

The same effect of mass vaporization can be observed on the gas phase density as shown in figure (5.5) . In the near injector region the density is very high and as the superheat decreases, the density reaches a stable state of $0.78kg/m^3$ for LN_2 and $1.03kg/m^3$ for LO_x, which is the satutration condition state corresponding to the prevailing pressure in the chamber.

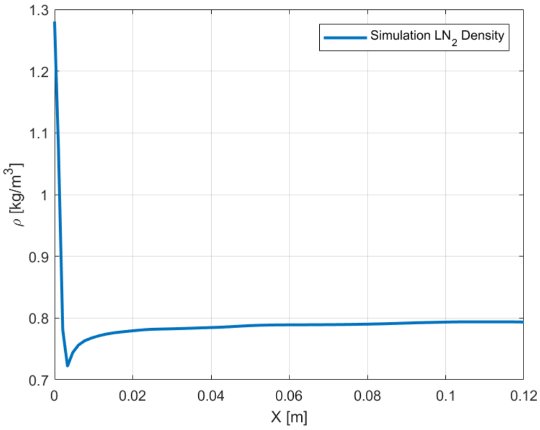

(a) LN_2 Gas Phase Density (b) LO_x Gas Phase Density

Figure 5.5.: Effects of Mass Vaporization on Gas Phase Density

5.2.2. Validation

Spray pattern captured with schlieren photography and the measured spray temperature are used for the validation of the simulation. In figure (5.6) a direct camparison of simulation with experiment is shown. As one can see, the simulation reproduces the spray charachteristics of a superheated spray very well. After the injection into the low pressure environment a rapid depressurization takes place. This leads to massive mass vaporization and expansion of the spray, which results in increasing of the spray angel. In both cases in the experiment and in the simulation most of mass vaporization due to flashing happens in the near injector region. Therefore the highest increasement of the spray angel is in this region.

Comparing the LN_2 spray with LO_x spray the influence of superheat on the spray expansion becomes abvious. Since the LO_x spray is more superheated ($\Delta T = 42K$). It undergoes higher expansion and reaches almost the chamber wall as compared to LN_2 spray ($\Delta T = 33$), which shows a slightly lower expansion. After 0.04 m in z direction most of the superheat has been consumed, which leads to less spray expansion and nearly a constant dropelts trajectory in the experiment and in the simulation for both sprays.

Furthmore the contribution of heat transfer from the surrounding via radiation and conduction to droplet mass vaporization is also evident in the simulation and in the experiment. The droplets in the outer region of the spray get more heat from the surrouding, which results in higher vaporization. This leads to higher expansion, less denser spray and smaller droplet diameter in the outer region of the spray.

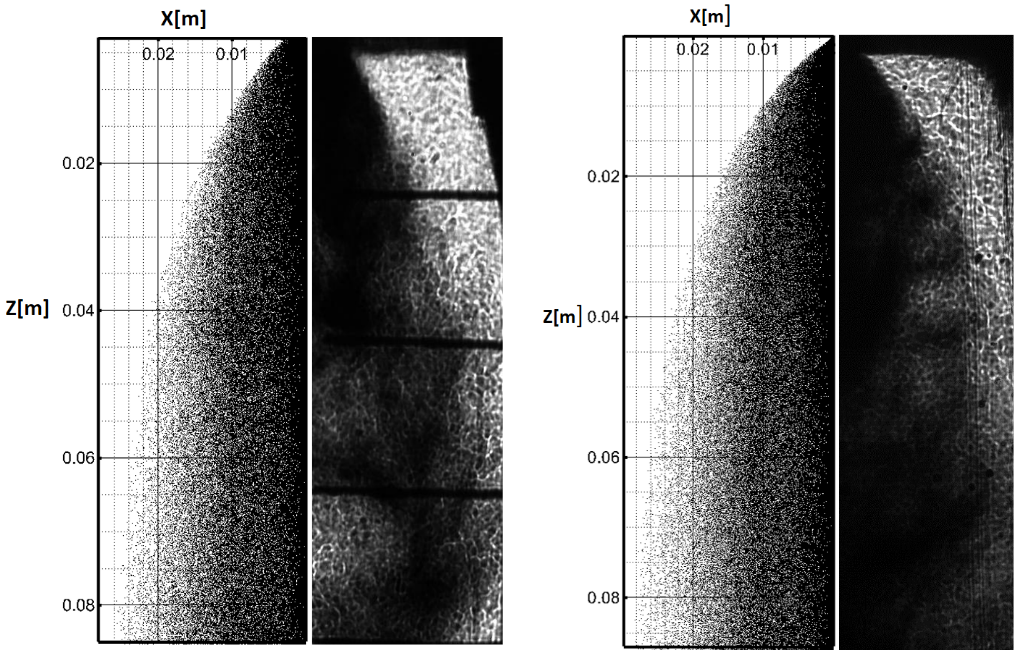

(a) LN_2 Spray

(b) LO_x Spray

Figure 5.6.: Comparison of Spray Pattern in Simulation with Experiment

After the injection in the low pressure chamber the spray gets superheated. Therefore a violent atomization and vaporization process takes place to reach a stable equilibrium state. As a result of this vaporization process the spray consumes more and more latent heat and causes an ambient temperature drop. Simutaneously the flash vaporization decreases the spray temperature, until a equilibrium state has been reached, which corresponds to the saturation condition according to the prevailing pressure in the chamber.

In figure (5.7) a comparison of temperature profile along the centerline is shown. Considering the prevailing pressure of 0.15 bar for the nitrogen case and 0.206 bar for the oxygen case a stable state has been reached with a temperature drop after injection to 64 K for nitrogen case and 77 K for oxygen case respectively. The measured temperature in the experiment is for nitrogen case about 65 K, which is about 1 K higher than the staturation temperature. This small error of 1 K in the experiment can occur using the thermocouples. For the oxygen case the measured temperature is 77 K, which is the saturation temperature at 0.206 bar.

As one can see in figure (5.7) the new implemented model is able to reproduce the results very accurately. In the nitorgen case the temperature drops directly after the injection to the saturation temperature of about 64 K. In the oxygen case a little error of about 5 K occurs in the near injector region, where the temperature in the simulation is about 82 K and the temperature in the experiment is 77 K. This small error is negible for a simulation.

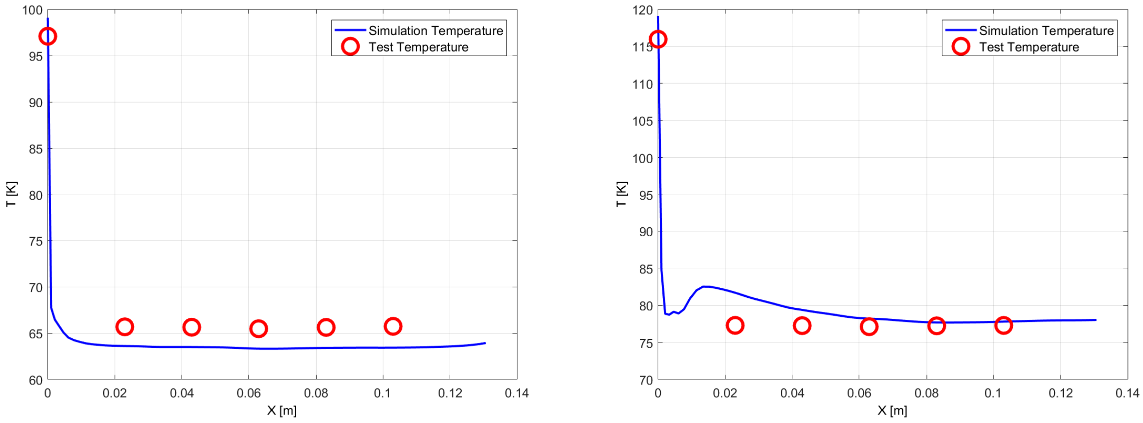

(a) LN_2 Spray

(b) LO_x Spray

Figure 5.7.: Temperature in Simulation and in Experiment along the Spray Centerline

In addition to the centerline temperature in figure (5.8) whole temperature profile of both cases is shown. As one can see the temperature sinks to the nearly saturation temperature as a result of consumption of latent heat in the spray region.

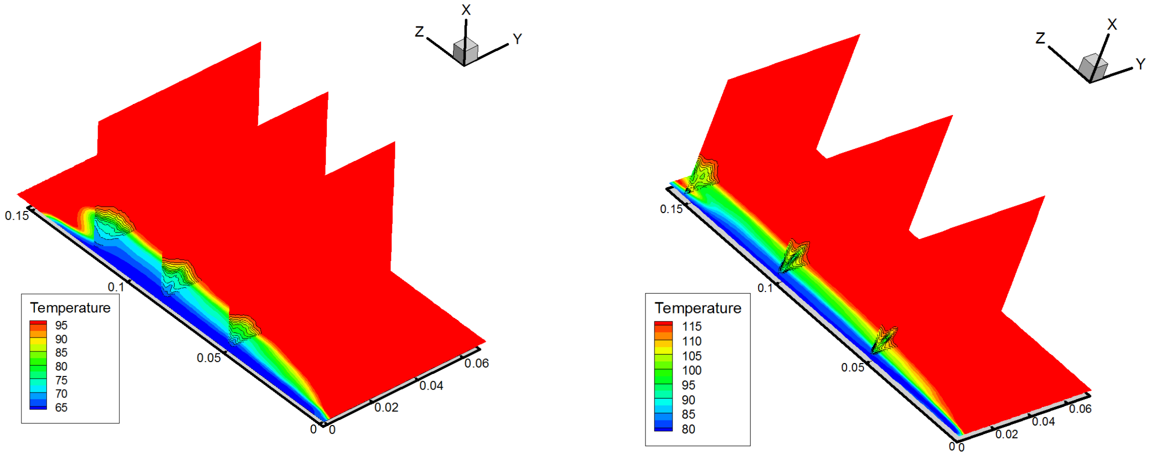

(a) LN_2 Spray Temperature

(b) LO_x Spray Temperature

Figure 5.8.: Temperature Distribution in the Simulation

A very good agreement is achieved between simulation results and the experimental results. The implemented code is able to reproduce all the charachterisitcs of a superheated spray. All the physical effects observed in the experiment for instance higher expansion of the spray with higher superheat, higher evporation in the near injector region and the measured temperature are predicted by the simulation very accurately. As previously mentioned the influence of high superheat on the expansion of the spray is evident through the comparision of LN_2 spray with LO_x spray in figure (5.6). Since the LO_x spray is more superheated. It expands wider in the experiment as well as in the simulation.

The Influence of radiative and conductive heat transfer from surrounding to the spray is abvious. Both results the experiment and the simulation show a denser spray with higher droplet size in the core region. While in the outer region of the spray, the droplets are smaller due to higher vaporization.

Furthermore the simulation shows the influence of the chosen droplet size on the angle and width of the spray. Besides these valdation cases, further simulation cases were conducted with uniform droplet diamter of 5-25 μm. Sprays with higher uniform droplet diameter have higher width, but the spray angle decreases with higher diameter. This effect can be explained with the inertia of the droplet. The bigger the droplet the higher is its interia, as a result it tends to remain its trajectory. The influence of the gas phase on droplet trajectory is lower for bigger droplets. In comparison to spray the smaller droplets show higher increase in the spray angle and expansion in the near injector region. But their width is smaller and their trajectory is influenced by the gas phase.

6. Conclusion

A numerical study is carrired out to investigate the cryogenic propellants flashing phenomenon. This phenomenon occurs in the space craft engines. When the pressurized propellant is injected into low pressure combustion chamber. A model according to Adachi et el [1] and Zuo et al [2] is implemented in Ansys Fluent. As compared to the model of Zuo et al, this new model considers the heat radiation from the surrounding for the droplet vaporization.

The simulation can successfully reproduce the results of the experiment. A very good agreement is achieved for the spray pattern and temperature. This flashing atomization model can be used for the simulation in combination of ignition and combustion of cryogenic propellants in low pressure environment.

Bibliography

[1] M.Adachi and V.McDonell, *Characterization of Fuel Vapor Concentration inside a Fuel Boiling Spray*. SAE Technical Paper, 1997.

[2] B.Zuo and A. Gomes, *Modelling superheated fuel sprays and vaporization*. International Journal of Engine Research, 2000.

[3] M.Luo and O.Haidn, *Injection of Cryogenic Propellants under Low Pressure Conditions*. 52nd AIAA/ASME/SAE/ASEE Joint Propulsion Conference, Salt Lake City,UT, 2016.

[4] A. Bakker, *Lecture Introduction into CFD, Fluent inc.* 2002.

[5] I. ANSYS, *ANSYS Fluent Theory Guide,Release 15.0*. 2013.

[6] O. M.Luo, *Injection of Cryogenic Propellants under Low Pressure Conditions*. 52nd AIAA/SAE/ASEE Joint Propulstion Conference,Salt Lake City, UT, 2016.

[7] R. Brown and L. York, *Spray Formed by Flashing Liquid Jets*. AICHE Journal., vol. 28, no.2, pp.149-153, 1962.

[8] D.Yildiz, *Experimental investigation of superheated liquid jet atomization due to flashing phenomena*. PhD thesis, Universite Libre de Bruxelles ULB, Belgium, 2005.

[9] J. Allen, *Laser-based measurements in tow-phase Flashing propane jets*. Journal of Loss Prevention in the Process Industries., vol. 11, no.5, pp.299-306, 1998.

[10] H. Y.Kitamura and T. T, *Critical superheat for Flashing of superheated liquid jet*. Ind.Eng. Chem.Fundam., vol. 25, no.2, pp.207-211, 1986.

[11] E. L.Nghiem, H.Merte and H.Beer, *Prediction of transient inception of boiling in terms of a heterogeneous nucleation theory*. Journal of Heat Transfer., vol. 103, no.1, 1981, 1981.

[12] B. Park and S.Lee, *An experimental investigation of the Flash atomization mechanism*. Atomization and Sprays., vol. 4, no.2, pp.159-179, 1994.

[13] H. G.Lamanna, B., and Weigand, *Towards a unified treatment of fully flashing spray*. International Journal of Multiphase Flow,., vol. 58, no.2, pp.168-184, 2013.

[14] V.Gautam and A. Gupta, *Fate of cryogenic fluid flow and atomization from a sheer coaxial injector under preignition conditions*. 44th AIAA/ASME/SAE/ASEE Joint Propulsion Conference and Exhibit, Hartford, 2008.

[15] S. Aggarwal and F. Peng, *A Review of Droplet Dynamics and Vaporization Modeling for Engineering Calculations*. Journal of Engineering for Gas Turbines and Power, vol.117,no.2,pp.453, 1995.

[16] R.Radespiel, *script of Lecture Turbulente Stroemungen, TU Braunschweig*. WS 14/15.

[17] I. ANSYS, *ANSYS Fluent UDF Manuel,Release 15.0*. 2013.

[18] Y. J. G.Lamanna, P.Rack, *Droplet sizing and infrared temperature measurments in superheated sprays*. 8th European Symposium on Aerothermodynamics for Space Vehicles,Lisbon,Portugal, 2015.

[19] R. Schmehl and J.Steeland, *Computational Analysis of the Oxidizer Preflow in an Upper-Stage Rocket Engine*. Journal of Propulsion and Power,vol.25,no.3, 2009.

[20] T.Ramcke and M.Pfitzner, *Simulation of Injection of LOX/GCH4 under Flashing Conditions*. 54th AIAA Aerospace Sciences Meeting,San Diego,California,USA, 2016.

[21] T.Ramcke and M.Pfitzner, *Numerical Simulation of Atomization and Flash Evaporation of Cryogenic Nitrogen Injection*. 8th Internation Symposium on Turbulence, Heat and Mass Transfer, 2015.

[22] B. Incropera, DeWitt, *Fundamentals of Heat and Mass Transfer*. John Wiley and Sons,6th Edition, 2006.

[23] J. R.S.Miller, K.Harstad, *Evaluation of equibrium and non-equilibrium evaporation models for many-droplet gas-liquid flow simulations*. International Journal of Multiphase Flow, 1998.

[24] O. M.Luo, T.Ramcke and M.Pfitzner, *Experimental and Numerical Investigation of Flash Atomization with Cryogenic Fluids*. 9th Internation Conference on Multiphase Flow, 2016.

[25] H. W. Vincent Cleary, Phil Brown, *Flashing liquid jets and two-phase droplet dispersion 1. Experiments for derivation of droplet atomization correlations*. Journal of Harzardous Materials, 2007.

[26] P. B. Henk Witlox, Mike Harper and V. Cleary, *Flashing liquid jets and two-phase droplet disperon II. Comparison and validation of droplet size and rainout formulations*. Journal of Harzardous Materials, 2007.

[27] R. U.Rana, *Design of Valve Segment for a Hybrid Rocket Engine*. Deutscher Luft-und Raumfahrtkongress, Augsburg, 2014.

[28] Y. L. Jon Paul Janet and D. Lucas, *Heterogeneous nucleation in CFD simulation of flashing flows in converging-diverging nozzles*. International Journal of Multiphase Flow,vol.74,pp106-117, 2015.

[29] H.Q.Yang and P.Dionne, *Modelling Porpellant Injection and Flash Atomization*. 47th AIAA Aerospace Sciences Meeting Including The New Horizons Forum and Aerospace Exposition,Orlando,Florida, 2009.

[30] N. A. Adams, *skriptum of Lecture Fluid Mechanics for Process Engineering, TU Munich.* WS 15/16.

[31] N. A. Adams, *script of Lecture Gas Dynamics, TU Munich.* SS 17.

[32] N. A. Adams, *script of Lecture of Applied CFD, TU Munich.* WS 15/16.

[33] N. A. Adams, *script of Lecture Numerical Calculation Methods of Turbulent Flows, TU Munich.* WS 16/17.

[34] NIST, *[Online] [Available:http://webbook.nist.gov/chemistry/fluid/], [Accessed:4.12.2017].*

[35] O. J. Haidn, *script of Lecture Raumfahrtantriebe 1, TU Munich.* WS 16/17.

[36] O. J. Haidn, *script of Lecture Raumfahrtantriebe 2, TU Munich.* SS 16.

[37] O. J. Haidn, *script of selected topics of space propulsion, TU Munich.* WS 16/17.

[38] M. .Raju, *CFD Modeling of Superheated Fuel Sprays.* 47th AIAA Aerospace Sciences Meeting Including The New Horizons Forum and Aerospace Exposition,Orlando,Florida, 2009.

[39] H. W. M. Witlox, *Flashing liquid jets and two phase dispersion.* HSE Books, 2002.

[40] A. E. H. Geanette Polanco and G. Munday, *General Review of Flashing jet studies.* Journal of Hazardous Materials,vol.173,pp2-18, 2012.

[41] L.-D. A.S.P.Solomon, *Investigation of Spray Characteristics for Flashing Injection of Fuels Containing Dissolved Air and Superheated Fuels.* NASA,NASA Contracter Report 3563, 1982.

A. Nomenclature

Latin symbols

$\dot{m}$	Mass vaporization rate	$[kg/s]$
m	Mass	$[kg]$
T	Temperature	$[K]$
L	Latent heat	$[J/kg]$
A	Area	[m^2]
h	Enthalpy	[J/kg]
Nu	Nusselt number	[-]
p	Pressure	[bar]
k_B	Bolzmann constant	[J/K]
v	specific volume	$[m^3]$
Re	Reynolds number	[-]
ΔG^*	Nucleation barrier	[J]
Pr	Prandtl number	[-]
B_T	Spalding heat transfer number	[-]
F_T	Correctin factor	[-]
R_p	Superheat parameter	[K]
ΔT	Superheat level	[K]
c_p	Specific heat	$[J/kgK]$
d	Droplet diameter	[m]
r	Droplet radius	[m]
v	Velocity	$[m/s]$
t	Time	$[s]$
l	length	$[m]$
S_m	Mass source	$[kg/s]$

S_h	Energy source	$[W]$
F	Force	$[N]$
g	Gravitational accceleration	$[9.81m/\mathrm{s}^2]$
E	Energy	$[J]$
J	Mass flux; diffusion flux	$[kg/s]$
k	Turbulence kinetic energy	$[J/kg]$
C	Turbulence model constant	[-]
f	focal length	[m]

Greek symbols

α_s	Heat transfer coefficient	$[\mathrm{kJ/m^2K\ s}]$
λ	Thermal conductivity	$[W/mK]$
μ	Viscosity	$[\mathrm{kg/m\ s}]$
ρ	Density	$[kg/\mathrm{m}^3]$
ε	Turbulent dissipation rate	$[m^2/s^3]$
ω	Specific dissipation rate	$[1/s^{-3}]$
σ	Surface tension	$[\mathrm{mN/m}]$
σ	Stefan Boltzmann constant	$[W/m^2K^4]$
α	Absorption cofficient	[-]
ω	Specific dissipation rate	$[1/s^{-3}]$
χ	non-dimensional nucleatoin barrier	[-]
ξ	non-dimensional nucleation barrier	[-]

Subscript

c	Conductive
0	Initial
inj	Injection
sat	Saturation
b	Boiling
p	Particle
d	Droplet

ref	Reference
r	Radiative
f	Flashing
t	Total
∞	Surrounding
C	Continuous phase
d	Disperse phase
c	Chamber
$wall$	Chamber wall

Abbreviations

LOX	Liquid oxygen
GOX	Gaseous oxygen
LN2	Liquid nitrogen
GN2	Gaseous oxygen
CFD	Computational fluid dynamics
SMD	Sauter mean diameter
RANS	Reynols-averged Navier-Stokes equations
URANS	Unsteady Reynols-averged Navier-Stokes equations
DNS	Direct numerical simulation
LES	Large eddy simulation
UDF	User defined function
DPM	Discrete phase model

B. Flash Atomization User Defined Functions

B.0.1. Nitrogen case UDF

```
#include "udf.h"
#include "dpm.h"

/*The following law determines how the droplet loses
 its mass and temperature.This law determine the properties
of a droplet e.g diameter,density,mass,temperature
etc for a single droplet! */

DEFINE_DPM_LAW(Flashing_Evaporation_Law,p,ci)
{
Material*m = P_MATERIAL(p);
cell_t c = P_CELL(p);
Thread *t = P_CELL_THREAD(p);
real Temp_c=C_T(c,t);
real dens_c= C_R(c,t);
real alpha;
real Pr;
real Re;
real Nu0;
real Nu;
real BT;
real FT;
real m_dot_flash;
real m_dot_con;
real m_dot_res;
real mp=P_MASS(p);
real Tp=P_T(p);
real Dp=P_DIAM(p);
real Ap=DPM_AREA(Dp);
real deltahv=DPM_LATENT_HEAT(p,m);
real Tb=DPM_BOILING_TEMPERATURE(p,m);
real cp_d = DPM_SPECIFIC_HEAT(p,Tp);
real ra=(Dp/2);
real deltaT=Tp−Tb;
real v_p= P_VEL(p)[2];
real hb=−3.5918e−05*pow(Tb,4)+0.015703*pow(Tb,3)
−2.6332*pow(Tb,2)+1243.4*Tb−6806.3;
int n;
int k=1;
int l=1;
real a;
real b;
real xn;
real fx;
real dfx;
real tol;
real xneu;
real abserror;
real guess;
real xn1;
real fc;
real fxl;
real cc;
real xl=1e−15;
real xu=1e−10;
real rho;
real Er;
real m_dot_r;
real Tem_wall=230;

/* Calculation of gas phase properties at reference temperature*/

real Tem_ref= (1./3.)*Temp_c+(2./3.)*Tb;
real mu_reference= 1.5049e−15*pow(Tem_ref,4)−5.8632e−13*pow(Tem_ref,3)
+1.5584e−11*pow(Tem_ref,2)+7.4642e−08*Tem_ref−2.7166e−07;
real ktc_reference=2.9923e−12*pow(Tem_ref,4)−1.3097e−09*pow(Tem_ref,3)
+1.371e−07*pow(Tem_ref,2)+9.6886e−05*Tem_ref−0.00075523;
real cp_reference = 2.9982e−06*pow(Tem_ref,4)−0.0012842*pow(Tem_ref,3)
+0.20861*pow(Tem_ref,2)−15.355*Tem_ref+1477.9;
real h_amb=−1.8389e−05*pow(Temp_c,4)+0.0091613*pow(Temp_c,3)
−1.7342*pow(Temp_c,2)+1189.5*Temp_c−5622.1;
Pr=mu_reference*cp_reference/ktc_reference;
Re=dens_c*v_p*Dp/mu_reference;
Nu0=2.0+0.552*( sqrt(Re))*pow(Pr,1./3.);
BT=cp_reference*(Temp_c−Tb)/deltahv;
```

```
FT=pow((1+BT),0.7)*log(1+BT)/BT;
Nu=2+(Nu0-2)/FT;
a=(2*M_PI*ktc_reference/cp_reference)*ra*Nu;
b= (h_amb-hb)/deltahv;


/*Superheat coffecient according to Adachi's correlation*/

if (deltaT >= 25)
 {alpha=13.8*pow(deltaT, 0.39); }
else if (5 < deltaT && deltaT < 25)
 {alpha= 0.027*pow(deltaT, 2.33);}
else if (0 < deltaT && deltaT <=5)
{alpha= 0.76*pow(deltaT, 0.26); }

/* Calculation of mass vaporization due to internal superheat
 Flashing (m_dot_con) */

m_dot_flash=Ap*alpha*deltaT/(deltahv/1000);

/* Calculation of mass vaporization due to heat conduction from
 surrounding (m_dot_con) */
/* First step-> Bisection method for finding the initial guess for fixed
point iteration method*/

for (k;k<5;k++)
{
 cc=(xl+xu)/2;
 fxl=-xl+a/(1+m_dot_flash/xl)*log(1+(1+m_dot_flash/xl)*b);
 fc=-cc+a/(1+m_dot_flash/cc)*log(1+(1+m_dot_flash/cc)*b);
 if ( fc == 0 )
{break;}
else if (fxl*fc < 0 )
{xu = cc; }
 else
 {xl = cc; }
 }
guess=cc;

/* Second Step-> Now use the guess from bisection method as the
 initial value for the fixed point iteration method*/
```

```
do
{
xneu=a/(1+m_dot_flash/guess)*log(1+(1+m_dot_flash/guess)*b);
     abserror = fabs(xneu-guess);
     guess=xneu;
} while (abserror>1e-17);
if(Temp_c>Tb)
{m_dot_con=xneu;}
else
{m_dot_con=0;}

// Calculation of mass vaporization due to raditon (m_dot_r)

m_dot_r=5.670367e-08*Ap*(1*pow(Tem_wall,4)-1*pow(Tb,4))/deltahv;

/* Determine the new particle mass, diameter and temperature*/

if ( P_MASS(p)> 0 && P_T(p)>Tb)
  { P_MASS(p)-=(m_dot_con+m_dot_flash+m_dot_r)*P_DT(p);
    P_T(p)-=m_dot_flash*deltahv/(cp_d*P_MASS(p))*P_DT(p);
    P_RHO(p) = 0.001407*pow(P_T(p),3)-0.15462*pow(P_T(p),2)
   +3.9662*P_T(p)+963.55-5.3157e-06*pow(P_T(p),4);
    P_DIAM(p)=pow(6.0*P_MASS(p)/ (P_RHO(p)*M_PI ), 1./3.);
    } }

/*Calculation of the temperature dependent properties of the droplet*/
 /* Determine the temperature dependent density of the droplet*/

DEFINE_DPM_PROPERTY(density,c,t,p,T)

{ real rho;
rho=-5.3157e-06*pow(T,4)+0.001407*pow(T,3)-0.15462*pow(T,2)+3.9662*T+963.55;
return rho;
}

/*Determine the temperature dependent specific heat capacity of the droplet*/

DEFINE_DPM_PROPERTY(droplet_cp,c,t,p,T)
{
real mp0= P_INIT_MASS(p);
real mp = P_MASS(p);
real Cp=0.00012705*pow(T,4)-0.035285*pow(T,3)+3.7947*pow(T,2)-184.1*T+5359.5;
```

```
p->enthalpy = Cp*(T-T_REF);
return Cp;
}

/*Determine the temperature dependent properties of the gas phase*/

/*Calculation of gas phase viscosity */

DEFINE_PROPERTY(cell_viscosity ,c,t)
{
real mu_new;
real Temp_c=C_T(c,t);
mu_new= 1.5049e-15*pow(Temp_c,4) -5.8632e-13*pow(Temp_c,3)
+1.5584e-11*pow(Temp_c,2)+7.4642e-08*Temp_c-2.7166e-07;
return mu_new;
}

/* Calculation of gas phase thermal conductivity */

DEFINE_PROPERTY(cell_thermalconductiviy ,c,t)
{
real ktc_new;
real Temp_ktc=C_T(c,t);
ktc_new=2.9923e-12*pow(Temp_ktc,4) -1.3097e-09*pow(Temp_ktc,3)
+1.371e-07*pow(Temp_ktc,2)+9.6886e-05*Temp_ktc -0.00075523;
return ktc_new;
}

/*Calculation of gas phase specific heat*/

DEFINE_SPECIFIC_HEAT(cp_gas,T,Tref,h,yi)
{real cp_new;
 cp_new= 2.9982e-06*pow(T,4) -0.0012842*pow(T,3)
+0.20861*pow(T,2) -15.355*T+1477.9;
         *h=cp_new*(T-Tref);
        return cp_new;}

/*The following udf define the source terms to the gas phase*/

DEFINE_DPM_SOURCE(dpm_source,c,t,S,strength,p)

{Material *m=P_MATERIAL(p);
```

```
 real z;
 int n2=0;
 real alpha;
 real m_dot_flash;
 real m_dot_res;
 real heatsource;
 real heatsource1;
 real Dp_entr = P_DIAM0(p);
 real Dp=P_DIAM(p);
 real P_rho=P_RHO(p);
 real Ap_entr = DPM_AREA(Dp_entr);
 real Tb = DPM_BOILING_TEMPERATURE(p,m);
 real Tp_entr = P_T0(p);
 real deltahv=DPM_LATENT_HEAT(p,m);
 real deltaT = Tp_entr-Tb;
 real Tp=P_T(p);
 real m_dot_con;
 real Temp_c=C_T(c,t);
 real cp_v = 2.9982e-06*pow(Temp_c,4)-0.0012842*pow(Temp_c,3)
+0.20861*pow(Temp_c,2)-15.355*Temp_c+1477.9;
 real cp_d = DPM_SPECIFIC_HEAT(p,Tp);
 real h_amb=-1.8389e-05*pow(Temp_c,4)+0.0091613*pow(Temp_c,3)
-1.7342*pow(Temp_c,2)+1189.5*Temp_c-5622.1;
 real h_amb_tref=-1.8389e-05*pow(T_REF,4)+0.0091613*pow(T_REF,3)
-1.7342*pow(T_REF,2)+1189.5*T_REF-5622.1;
 real h_amb_tb=-1.8389e-05*pow(Tb,4)+0.0091613*pow(Tb,3)-1.7342*pow(Tb,2)
+1189.5*Tb-5622.1;

/* Mass source to the gas phase*/

/*(The mass source of a single dropelt is the difference in mass between
 the entry  of droplet to a cell and exit from this cell)*/

/*Total mass source from a cell is mass source of single dropelt multiplied
by strength,which is number of particles/s in stream*/

m_dot_res=(P_MASS0(p) - P_MASS(p))*strength;
if (m_dot_res <= 0)
          {m_dot_flash=0;}
        else

/*Superheat coefficient according to adachi's correlation*/
```

```
{
if (deltaT >= 25)
 {alpha=13.8*pow(deltaT, 0.39);}
else if (5 < deltaT && deltaT < 25)
 {alpha= 0.027*pow(deltaT, 2.33);}
else if (0 < deltaT && deltaT <=5)
{alpha= 0.76*pow(deltaT, 0.26);}
m_dot_flash=Ap_entr*alpha*deltaT/(deltahv/1000)*strength*P_DT(p);}

/*Energy source term to the gas phase*/

heatsource=(P_MASS0(p)*cp_d*(P_T0(p)-T_REF)-cp_d*P_MASS(p)*(P_T(p)
-T_REF)-(P_MASS0(p)-P_MASS(p)
-m_dot_flash/strength)*P_INJECTION(p)->latent_heat_ref)*strength;

 /*Switching between the boiling law and Flash_Evaporation_Law*/

if (P_CURRENT_LAW(p) == DPM_LAW_USER_1)
{S->species [n2]+= m_dot_res;
S->mass = m_dot_res;
S->energy=heatsource;}
 }

/* Check If the particle temperature is higher than the
 boiling temperature
according to the gas phase pressure
If this condition applies-> switch to Flashing law*/

/*if not then use depending on the temperature the
boiling law or vaporitzation law*/

DEFINE_DPM_SWITCH(dpm_switch, p, coupled)
{
cell_t c = P_CELL(p);
Thread *t = P_CELL_THREAD(p);
Material *m = P_MATERIAL(p);
if ( P_T(p) > DPM_BOILING_TEMPERATURE(p, m))
P_CURRENT_LAW(p) = DPM_LAW_USER_1;
else
P_CURRENT_LAW(p) = DPM_LAW_BOILING;
}
```

B.0.2. Oxygen case UDF

```
#include "udf.h"
#include "dpm.h"

/* The following law determines how the droplet
 loses its mass and temperature*/

/* This law determines the properties of a droplet
 e.g diameter,density,mass,temperature etc for a single droplet!*/

DEFINE_DPM_LAW(Flashing_Evaporation_Law,p,ci)
{

Material*m = P_MATERIAL(p);
cell_t c = P_CELL(p);
Thread *t = P_CELL_THREAD(p);
real Temp_c=C_T(c,t);
real dens_c= C_R(c,t);
real alpha;
real Pr;
real Re;
real Nu0;
real Nu;
real BT;
real FT;
real m_dot_flash;
real m_dot_con;
real m_dot_res;
real mp=P_MASS(p);
real Tp=P_T(p);
real Dp=P_DIAM(p);
real Ap=DPM_AREA(Dp);
real deltahv=DPM_LATENT_HEAT(p,m);
real Tb=DPM_BOILING_TEMPERATURE(p,m);
real cp_d = DPM_SPECIFIC_HEAT(p,Tp);
real ra=(Dp/2);
real deltaT=Tp-Tb;
real v_p= P_VEL(p)[2];
real hb=9.6769e-06*pow(Tb,4)-0.082121*pow(Tb,3)
+15.491*pow(Tb,2)-90.222*Tb+21421;
```

```
int n;
int k=1;
int l=1;
real a;
real b;
real xn;
real fx;
real dfx;
real tol;
real xneu;
real abserror;
real guess;
real xn1;
real fc;
real fxl;
real cc;
real xl=1e-15;
real xu=1e-10;
real rho;
real Er;
real m_dot_r;
real Tem_wall=230;

/* Calculation of gas phase properties
at reference temperature*/

real Tem_ref= (1./3.)*Temp_c+(2./3.)*Tb;
real mu_reference= 1.8542e-16*pow(Tem_ref,4)
-6.8643e-14*pow(Tem_ref,3)-5.6412e-11*pow(Tem_ref,2)
+8.8871e-08*Tem_ref-5.6932e-07;
real ktc_reference=4.1868e-13*pow(Tem_ref,4)
-2.6237e-10*pow(Tem_ref,3)+8.0071e-09*pow(Tem_ref,2)
+0.00010188*Tem_ref-0.0010885;
real cp_reference = 5.5376e-07*pow(Tem_ref,4)
-0.00037957*pow(Tem_ref,3)+0.094696*pow(Tem_ref,2)
-10.153*Tem_ref+1304.2;
real h_amb=4.0786e-07*pow(Tem_ref,4)-0.0001704*pow(Tem_ref,3)
+0.012296*pow(Tem_ref,2)+913.19*Tem_ref-829.35;
Pr=mu_reference*cp_reference/ktc_reference;
Re=dens_c*v_p*Dp/mu_reference;
Nu0=2.0+0.552*( sqrt(Re))*pow(Pr,1./3.);
BT=cp_reference*(Temp_c-Tb)/deltahv;
```

```
FT=pow((1+BT),0.7)*log(1+BT)/BT;
Nu=2+(Nu0-2)/FT;
a=(2*M_PI*ktc_reference/cp_reference)*ra*Nu;
b= (h_amb-hb)/deltahv;


/*Superheat coffecient according to Adachi's correlation*/

if (deltaT >= 25)

{alpha=13.8*pow(deltaT, 0.39); }

else if (5 < deltaT && deltaT < 25)

{alpha= 0.027*pow(deltaT, 2.33);}

else if (0 < deltaT && deltaT <=5)

{alpha= 0.76*pow(deltaT, 0.26); }


/* Calculation of mass vaporization due to internal
superheat ->Flashing (m_dot_con) */

m_dot_flash=Ap*alpha*deltaT/(deltahv/1000);


/* Calculation of mass vaporization due to heat conduction
 from surrounding (m_dot_con) */


/* First step-> Bisection method for finding the initial
guess for fixed point iteration method*/

for (k;k<5;k++)
{
 cc=(xl+xu)/2;
 fxl=-xl+a/(1+m_dot_flash/xl)*log(1+(1+m_dot_flash/xl)*b);
 fc=-cc+a/(1+m_dot_flash/cc)*log(1+(1+m_dot_flash/cc)*b);
 if ( fc == 0 )
{break;}
else if (fxl*fc < 0 )
{xu = cc; }
 else
 {xl = cc; }
 }
guess=cc;

/* Second Step-> Now use the guess from bisection
method as the initial value for the fixed point iteration method*/

do
{neu=a/(1+m_dot_flash/guess)
*log(1+(1+m_dot_flash/guess)*b);
    abserror = fabs(xneu-guess);
    guess=xneu;
} while (abserror>1e-17);

if(Temp_c>Tb)
{m_dot_con=xneu;}
else
{m_dot_con=0;}


// Calculation of mass vaporization due to raditon (m_dot_r)

m_dot_r=5.670367e-08*Ap*(1*pow(Tem_wall,4)
-1*pow(Tb,4))/deltahv;

/* Determine the new particle mass, diameter and temperature*/

if ( P_MASS(p)> 0 && P_T(p)>Tb)

{    P_MASS(p)-=(m_dot_con+m_dot_flash+m_dot_r)*P_DT(p);
     P_T(p)-=m_dot_flash*deltahv/(cp_d*P_MASS(p))*P_DT(p);
     P_RHO(p)=-1.2945e-05*pow(Tp,4)+0.0048875*pow(Tp,3)
-0.69914*pow(Tp,2)+39.693*Tp+518.69;
     P_DIAM(p)=pow(6.0*P_MASS(p)/ (P_RHO(p)*M_PI ), 1./3.);}}

/*Calculation of the temperature dependent
 properties of the droplet*/

 /* Determine the temperature dependent density of the droplet*/
```

```
DEFINE_DPM_PROPERTY(density,c,t,p,T)
{ real rho;
rho=-1.2945e-05*pow(T,4)+0.0048875*pow(T,3)
-0.69914*pow(T,2)+39.693*T+518.69;
return rho;
}

/*Determine the temperature dependent specific
 heat capacity of the droplet*/

DEFINE_DPM_PROPERTY(droplet_cp,c,t,p,T)
{
real mp0= P_INIT_MASS(p);
real mp = P_MASS(p);
real Cp=0.00060785*pow(T,4)-0.24247*pow(T,3)
+35.77*pow(T,2)-2305.9*T+56387;
p->enthalpy = Cp*(T-T_REF);
return Cp;}

/*Determine the temperature dependent
properties of the gas phase*/

/*Calculation of gas phase viscosity */

DEFINE_PROPERTY(cell_viscosity,c,t)
{
real mu_new;
real Temp_c=C_T(c,t);
mu_new= 1.8542e-16*pow(Temp_c,4)
-6.8643e-14*pow(Temp_c,3)-5.6412e-11*pow(Temp_c,2)
+8.8871e-08*Temp_c-5.6932e-07;
return mu_new;}

/* Calculation of gas phase thermal conductivity */

DEFINE_PROPERTY(cell_thermalconductiviy,c,t)
{real ktc_new;
real Temp_ktc=C_T(c,t);
ktc_new=4.1868e-13*pow(Temp_ktc,4)
-2.6237e-10*pow(Temp_ktc,3)+8.0071e-09*pow(Temp_ktc,2)
+0.00010188*Temp_ktc-0.0010885;
return ktc_new;}
```

```
/*Calculation of gas phase specific heat*/
DEFINE_SPECIFIC_HEAT(cp_gas,T,Tref,h,yi)
       {real cp_new;
cp_new= 5.5376e-07*pow(T,4)-0.00037957*pow(T,3)
+0.094696*pow(T,2)-10.153*T+1304.2;
 *h= cp_new*(T-Tref);
   return cp_new;}

/*The following udf define the source terms to the gas phase*/

DEFINE_DPM_SOURCE(dpm_source,c,t,S,strength,p)
{Material *m=P_MATERIAL(p);
 real z;
 int n2=0;
 real alpha;
 real m_dot_flash;
 real m_dot_res;
 real heatsource;
 real heatsource1;
 real Dp_entr = P_DIAM0(p);
 real Dp=P_DIAM(p);
 real P_rho=P_RHO(p);
 real Ap_entr = DPM_AREA(Dp_entr);
 real Tb = DPM_BOILING_TEMPERATURE(p,m);
 real Tp_entr = P_T0(p);
 real deltahv=DPM_LATENT_HEAT(p,m);
 real deltaT = Tp_entr-Tb;
 real Tp=P_T(p);
 real m_dot_con;
 real Temp_c=C_T(c,t);
 real cp_v = 0.00091735*pow(Temp_c,4)-0.366*pow(Temp_c,3)
+54.007*pow(Temp_c,2)-3484.1*Temp_c+83744;
 real cp_d = DPM_SPECIFIC_HEAT(p,Tp);

 /* Mass source to the gas phase*/
/*(The mass source of a single dropelt is the difference
 in mass between the entry  of droplet to a cell and exit
 from this cell)*/
/*Total mass source from a cell is mass source of single
 dropelt multiplied by strength,which is number of particles/s in stream*/
m_dot_res=(P_MASS0(p) - P_MASS(p))*strength;

if (m_dot_res <= 0)
        {m_dot_flash=0;}
else
/*Superheat coefficient according to adachi's correlation*/
{if (deltaT >= 25)
 {alpha=13.8*pow(deltaT, 0.39);}
else if (5 < deltaT && deltaT < 25)
 {alpha= 0.027*pow(deltaT, 2.33);}
else if (0 < deltaT && deltaT <=5)
{alpha= 0.76*pow(deltaT, 0.26);}
m_dot_flash=Ap_entr*alpha*deltaT/(deltahv/1000)
*strength*P_DT(p);}

/*Energy source term to the gas phase*/

heatsource=(P_MASS0(p)*cp_d*(P_T0(p)-T_REF)
-cp_d*P_MASS(p)*(P_T(p)-T_REF)-(P_MASS0(p)-P_MASS(p)
-m_dot_flash/strength)*P_INJECTION(p)->latent_heat_ref)*strength;

/*Switching between the boiling law and Flash_Evaporation_Law*/
if (P_CURRENT_LAW(p) == DPM_LAW_USER_1)
{S->species [n2]+= m_dot_res;
S->mass = m_dot_res;
S->energy=heatsource;}}
/* Check If the particle temperature is higher than
the boiling temperature according to the gas phase pressure
/*If this condition applies-> switch to Flashing law*/
/*if not then use depending on the temperature the boiling
 law or vaporitzation law*/

DEFINE_DPM_SWITCH(dpm_switch, p, coupled)
{cell_t c = P_CELL(p);
Thread *t = P_CELL_THREAD(p);
Material *m = P_MATERIAL(p);
if ( P_T(p) > DPM_BOILING_TEMPERATURE(p, m))
P_CURRENT_LAW(p) = DPM_LAW_USER_1;
else
P_CURRENT_LAW(p) = DPM_LAW_BOILING;
}
```

B.0.3. Matlab Code for finding the initial guess for Bisection Method

Nitrogen Case

```
clc;
 clear all;
 close all;

initial values and boundary conditions
Tb=65;
deltahv=199000;
Tinj=94;
Tamb=100;
v_d=45;
p_amb=0.15;
droplet_d=30e-06;

Reference Temperaure

Tref=(2/3)*Tb+(1/3)*Tamb;

Calculation of gas properties at reference Temperature

cp=2.9982e-06*Tref^4-0.0012842*Tref^3
+0.20861*Tref^2-15.355*Tref+1477.9;
ktc=2.9923e-12*Tref^4-1.3097e-09*Tref^3+
1.371e-07*Tref^2+9.6886e-05*Tref-0.00075523;
mu=1.5049e-15*Tref^4-5.8632e-13*Tref^3
+1.5584e-11*Tref^2+7.4642e-08*Tref-2.7166e-07;
hb=-3.5918e-05*Tb^4+0.015703*Tb^3-2.6332*Tb^2
+1243.4*Tb-6806.3;
hamb=-3.5918e-05*Tamb^4+0.015703*Tamb^3
-2.6332*Tamb^2+1243.4*Tamb-6806.3;
rho=9.5346e-09*Tamb^4-4.4002e-06*Tamb^3
+0.00080687*Tamb^2-0.07331*Tamb+3.2837  ;
Pr=(mu*cp)/ktc;


Reduction of superheat with intial delta T = 29 K
assuming delta T reduces 1K every time step

 for k=1:29
 Tinjneu(k)=94-k;
  deltat(k)=(Tinjneu(k)-Tb);

  if (deltat(k)>= 25)
      alpha(k)=13.8*((deltat(k))^0.39);
   elseif  (5<=deltat(k)<25)
      alpha(k)=0.027*((deltat(k))^2.33);
      else
     alpha(k)=0.76*((deltat(k))^0.26);
         end

Radius reduction of the dropet every time step

  red=((droplet_d)/2)/29;
  r(k)=(droplet_d/2)-(k*red);

Area of the droplets at every time step

A(k)=4*pi*r(k)^2;

Mass vaporization due to flashing

mflash(k)=(A(k)*alphaneu(k)*1000*(deltat(k)))/deltahv;

Calculating reynolds number, nusselt number, transfer number and FT

Re(k)=(rho*v_d*(2*r(k)))/mu;

Standard nusselt number

Nuo(k)=2+0.552*((Re(k)^1/2)*Pr^1/3);

Bt=(cp*(Tamb-Tb))/deltahv;

Ft=((1+Bt)^0.7)*(log(1+Bt)/Bt);
 Modified nusselt number
Nu(k)=2+((Nuo(k)-2)/Ft);

Guess for a good initial values for the Bisection method
xl=0.15e-19;   upper guess
xu=0.25e-10;   lower guess
```

```
up(k)=-xu+((2*pi*(ktc/cp)*r(k))*(Nu(k)/(1+(mflash(k)/xu)))
*(log(1+(1+(mflash(k)/xu))*(((hamb-hb)/deltahv)))));
low(k)=-xl+((2*pi*(ktc/cp)*r(k))*(Nu(k)/(1+(mflash(k)/xl)))
*(log(1+(1+(mflash(k)/xl))*(((hamb-hb)/deltahv)))));
 end

  Bisection method for finding the initial valure for fixed point iteration
  for l=1:29;
xl=1e-15;  upper guess
xu=1e-10;  lower guess
   r1=r(l);
   Nu1=Nu(l);
   mflash1=mflash(l);
        for u=1:20;
         c=(xl+xu)/2;
fxl=-xl+((2*pi*(ktc/cp)*r(k))*(Nu1/(1+(mflash(k)/xl)))
*(log(1+(1+(mflash(k)/xl))*(((hamb-hb)/deltahv)))));
fc=-c+((2*pi*(ktc/cp)*r1)*(Nu1/(1+(mflash1/c)))
*(log(1+(1+(mflash1/c))*(((hamb-hb)/deltahv)))));
  if ( fc == 0 )
          break;
   elseif (fxl*fc < 0 )
          xu = c;
      else
          xl = c;
end
 end
mitt(l)=c;   initial guesses for the fixed iteration method
end

Fixed point iteration method

for we=1:29
r12=r(we);
      Nu12=Nu(we);
      mflash12=mflash(we);
      mitt2=mitt(we);

for er=1:80
      tol=1e-60;
      x1=((2*pi*(ktc/cp)*r12)*(Nu12/(1+(mflash12/mitt2)))
   *(log(1+(1+(mflash12/mitt2))*(((hamb-hb)/deltahv)))));
```

```
    abserror=abs(x1-mitt2);

    if (abserror<tol)
            break
          end
    mitt2=x1;
end

Mass vaporization due to heat conduction
mittneu(we)=mitt2;
end

check, whether the found values for the root are good
best case if the variable 'zero' is 0 for every time step

for  tr=1:29
  r13=r(tr);
    Nu13=Nu(tr);
    mflash13=mflash(tr);
    mitt3=mittneu(tr);

 zero(tr)=-mitt3+((2*pi*(ktc/cp)*r13)*(Nu13/(1+(mflash13/mitt3)))
*(log(1+(1+(mflash13/mitt3))*(((hamb-hb)/deltahv)))));
  end

plot of the droplet mass evaporation due to flashing

figure
plot(deltat,mflash)
title('Droplet mass evaporation due to flashing')
xlabel('{\Delta} T [K]')
ylabel('mdot-flash [kg/s]')

plot of the droplet mass evaporation due to heat conduction
figure
plot(deltat,mittneu)
title('Droplet mass evaporation due to heat conduction')
xlabel('{\Delta} T [K]')
ylabel('mdot-con [kg/s]')

total mass evaporation including flashing and heat conduction
mres=mittneu+mflash;
```

```
plot of total droplet mass evaporation
figure
plot(deltat,mres);
title('total droplet mass evaporation');
xlabel('{\Delta} T [K]');
ylabel('mdot-result [kg/s]');
```

Oxygen Case

```
clc;
 clear all;
 close all;

initial values boundary condition
Tb=73;
deltahv=217000;
Tinj=97;
Tamb=100;
v_d=45;
p_amb=0.110;
droplet_d=30e-06;

Reference Temperature
Tref=(2/3)*Tb+(1/3)*Tamb;

Calculation of gas properties at reference Temperature

hb=9.6769e-06*Tb^4-0.082121*Tb^3+15.491*Tb^2
-90.222*Tb+21421;
cp= 5.5376e-07*Tref^4-0.00037957*Tref^3+
0.094696*Tref^2-10.153*Tref+1304.2;
ktc=4.1868e-13*Tref^4-2.6237e-10*Tref^3
+8.0071e-09*Tref^2+0.00010188*Tref-0.0010885;
mu= 1.8542e-16*Tref^4-6.8643e-14*Tref^3
-5.6412e-11*Tref^2+8.8871e-08*Tref-5.6932e-07;
hamb=4.0786e-07*Tref^4-0.0001704*Tref^3
+0.012296*Tref^2+913.19*Tref-829.35;
rho =9.4899e-101*Tamb^4-6.8501e-07*Tamb^3
+0.00019183*Tamb^2-0.02597*Tamb+1.6936;
Pr=(mu*cp)/ktc;

Simulating the reduction of superheat with intial delta T=29 K
Assumption the superheat reduces 1K every time step

for k=1:24

Tinjneu(k)=97-k;
   deltat(k)=(Tinjneu(k)-Tb);
       if (deltat(k)>= 25)
       alpha(k)=13.8*((deltat(k))^0.39);
      elseif  (5<=deltat(k)<25)
       alpha(k)=0.027*((deltat(k))^2.33);
         else
       alpha(k)=0.76*((deltat(k))^0.26);
          end

Radius reduction of the dropet every time step
   red=((droplet_d)/2)/29;
   r(k)=(droplet_d/2)-(k*red);

Area of the droplets at every time step
  A(k)=4*pi*r(k)^2;

mass vaporization due to flashing
  mflash(k)=(A(k)*alphaneu(k)*1000*(deltat(k)))/deltahv;

Calculating reynolds number, nusselt number, transfer number and FT
   Re(k)=(rho*v_d*(2*r(k)))/mu;

Standard nusselt number
 Nuo(k)=2+0.552*((Re(k)^1/2)*Pr^1/3);
 Bt=(cp*(Tamb-Tb))/deltahv;
 Ft=((1+Bt)^0.7)*(log(1+Bt)/Bt);

Modified Nusselt number
 Nu(k)=2+((Nuo(k)-2)/Ft);



Guess for a good initial value for the Bisection method
 xl=1e-15;   upper guess    change it according to the
 boundary conditions   very important
 xu=1e-10;   lower guess     change it according to the
 boundary condtions    very important

up(k)=-xu+((2*pi*(ktc/cp)*r(k))*(Nu(k)/(1+(mflash(k)/xu)))*
(log(1+(1+(mflash(k)/xu))*(((hamb-hb)/deltahv)))));
low(k)=-xl+((2*pi*(ktc/cp)*r(k))*(Nu(k)/(1+(mflash(k)/xl)))
*(log(1+(1+(mflash(k)/xl))*(((hamb-hb)/deltahv)))));
end

Bisection method for finding the initial valure for fixed point iteration
```

```
 for l=1:24;
  xl=1e-15; upper guess
  xu=1e-10;  lower guess
  r1=r(l);
  Nu1=Nu(l);
  mflash1=mflash(l);
  for u=1:20;
  c=(xl+xu)/2;

fxl=-xl+((2*pi*(ktc/cp)*r(k))*(Nu1/(1+(mflash(k)/xl)))
*(log(1+(1+(mflash(k)/xl))*(((hamb-hb)/deltahv)))));
fc=-c+((2*pi*(ktc/cp)*r1)*(Nu1/(1+(mflash1/c)))
*(log(1+(1+(mflash1/c))*(((hamb-hb)/deltahv)))));
 if ( fc == 0 )
       break;
       elseif (fxl*fc < 0 )
       xu = c;
      else
       xl = c;
end
end

mitt(l)=c; initial guesses for the fixed iteration method
end

Fixed point iteration method
  for we=1:24
    r12=r(we);
    Nu12=Nu(we);
    mflash12=mflash(we);
    mitt2=mitt(we);

for er=1:80
    tol=1e-60;
    x1=((2*pi*(ktc/cp)*r12)*(Nu12/(1+(mflash12/mitt2)))
   *(log(1+(1+(mflash12/mitt2))*(((hamb-hb)/deltahv)))));
    abserror=abs(x1-mitt2);
    if (abserror<tol)
             break
end
    mitt2=x1;
end
```

```
Mass vaporization due to heat conduction
mittneu(we)=mitt2;
end

check, whether the found values for the root are good
best case if the variable 'zero' is 0 for every time step
for  tr=1:24
  r13=r(tr);
  Nu13=Nu(tr);
    mflash13=mflash(tr);
    mitt3=mittneu(tr);
    zero(tr)=-mitt3+((2*pi*(ktc/cp)*r13)*(Nu13/(1+(mflash13/mitt3)))
   *(log(1+(1+(mflash13/mitt3))*(((hamb-hb)/deltahv)))));
    end
plot of the droplet mass evaporation due to flashing

figure
plot(deltat,mflash,'black')
title('Droplet mass evaporation due to flashing')
xlabel('{\Delta} T [K]')
ylabel('mdot-flash [kg/s]')

plot of the droplet mass evaporation due to heat conduction
figure
plot(deltat,mittneu,'black')
title('Droplet mass evaporation due to heat conduction')
xlabel('{\Delta} T [K]')
ylabel('mdot-con [kg/s]')

total mass evaporation including flashing and heat conduction
mres=mittneu+mflash;

plot of total droplet mass evaporation
figure
plot(deltat,mres,'black');
title('total droplet mass evaporation');
xlabel('{\Delta} T [K]');
ylabel('mdot-result [kg/s]');
```